2014

AROMATICITY RULES IN THE DEVELOPMENT OF NEGATIVE IONS

Brandon Child
Virginia Commonwealth University

AROMATICITY RULES IN THE DEVELOPMENT OF NEGATIVE IONS

A thesis submitted in partial fulfillment of the requirements for a degree of Master of Science, at Virginia Commonwealth University.

By

Brandon Child

M.S in Physics

Virginia Commonwealth University 2014

Director: Dr. Purusottam Jena, Distinguished Professor, Department of Physics

Virginia Commonwealth University
Richmond, Virginia

May 2014

Acknowledgement

I would first like to thank Dr. Purusottam Jena, whose compassion for the field was infectious, leading me to wonders I could have never found on my own. His guidance and understanding made this work possible, I could not have asked for better patronage. I would also like to thank Dr. Gronert whose advice helped start me down the right path.

I would like to thank all of my lab mates and class mates who were mutual moral support and study partners, in particular Rosie, Santanab, Jien, Chris, Alex, Tommy, Tyler, and Nilanta.

I would like to thank all my friends and family who supported and believed in me even during times of struggle and uncertainty.

I would like to thank Michelle who's compassion, support, understanding and caring I could not have survived these two years without.

Table of Contents

List of Tables

List of Figures

Abstract

AROMATICITY RULES IN THE DEVELOPMENT OF NEGATIVE IONS

By Brandon Child, M.S.

A thesis submitted in partial fulfillment of the requirements for a degree of Master of Science, at Virginia Commonwealth University.

Virginia Commonwealth University, 2014

Director: Dr. Purusottam Jena, Distinguished Professor, Department of Physics

Organic molecules are known for their stability due to aromaticity. Superhalogens, on the other hand, are highly reactive anions, whose electron affinity is larger than that of chlorine. This thesis, using first principles calculations, explores possible methods for creation of superhalogen aromatic molecules while attempting to also develop a fundamental understanding of the physical properties behind their creation. The first method studied uses anionic cyclopentadienyl and enhances its electron affinity through ligand substitution or ring annulation in combination with core substitutions. The second method studies the possibilities of using benzene, which has a negative electron affinity (EA), as a core to attain similar results. These cases resulted in EAs of 5.59 eV and 5.87 eV respectively, showing that aromaticity rule can be used to create strong anionic organic molecules. These studies will hopefully lead to new advances in the development of organic based technology.

Introduction

1.1 Overview

Superhalogens are a class of molecules whose electron affinities are larger than that of any halogen atom. As a result, superhalogens not only form stable salts but, due to the strong oxidizing properties of their parent species, also play a major role in the synthesis of new compounds. Consequently, there is a growing interest in a fundamental understanding of the structure, stability, and properties of these molecules, and in finding ways to enlarge their scope. For example, superhalogens were originally conceived[1] to have a metal atom, M, at their core surrounded by halogen atoms, X, whose number exceed the maximal valence, *k*, of the metal atom by one, namely MX_{k+1}. In the 1980's and 1990's many superhalogens were designed by considering simple metal atoms (M=Li, Na, Mg, Al, ...) at the core, and halogen atoms (X=F, Cl) as ligands[2,3,4,5]. The first experimental proof of superhalogens came from Wang's group in 1999[6]. Since then, a considerable amount of work has been done to design and synthesize new superhalogens and understand their atomic structure and properties[7,8,9,10,11,12,13]. These include new superhalogens with transition metal atoms at the core[14], and/or O, NO_3, CN, BH_4, and BF_4 moieties as ligands[15,16,17,18,19]. Superhalogens such as borane derivatives that contain neither a metal nor a halogen atom have also been designed[20]. In addition, it was recently shown[21] that a new class of highly electronegative ions can form if superhalogens, instead of halogens, are used as ligands. This new species, called hyperhalogens, have electron affinities larger than that of their superhalogen building blocks and open the door to the synthesis of powerful oxidizing

agents. Recent works have shown that these highly electronegative ions can be used to oxidize water[22], as well as increase the oxidation state of metal atoms[23].

1.2 Motivation

Electron counting rules[24] have played a significant role in the design and synthesis of many of the recently discovered super- and hyperhalogens. Commonly used rules are the octet rule, 18-electron rule, and the Wade-Mingos rule. The octet rule which requires that for a molecule to be stabilized or an atom to be chemically inert, the outer *s* and *p* valence electrons must be completely full ($s^2\ p^6$). This rule normally applies to light elements with atomic numbers less than 20. Since halogen atoms have an outer electron configuration of $s^2\ p^5$, only one electron is needed to complete the shell closing, and hence they possess large electron affinities. The 18-electron rule, on the other hand, applies to molecules containing transition metal elements, and requires s^2, p^6, and d^{10} orbitals to be full. As an example, consider $Au_{12}Ta$[25]; with Au and Ta respectively contributing 1 and 5 valence electrons each, $Au_{12}Ta$ has 12+5=17 outer electrons and needs only one electron to satisfy the 18-electron rule. Hence, its electron affinity should be high, and this has been confirmed experimentally[25]. It has also been shown that the Wade-Mingos rule which requires (n+1) pairs of electrons for stable cage-bonding can be used to design superhalogens. An example in this category is borane derivatives. Borane molecules forming polyhedral cages with *n* vertices have the formula $B_nH_n^{2-}$. Thus, if one can replace one B atom by a C atom or add one extra H atom to $B_nH_n^{2-}$, the corresponding molecules $CB_{n-1}H_n$ or B_nH_{n+1} would require only one electron to satisfy the Wade-Mingos rule. These rules have led to molecules with predicted electron affinities as high as 14 eV[26], although the highest confirmed experimentally has been around 9 eV[27].

Until now, all of the known superhalogens have been inorganic in nature, and organic molecules with electron affinities even approaching those of halogen atoms are not known. The possibility that the aromaticity[28,29] rule that accounts for the stability of organic molecules can be used to design superhalogens could lead to new developments in the fields of organic catalysis and development of organic based technology.

1.3 Superhalogen behavior by core or ligand substitution in aromatic molecules using C_5H_5

Aromaticity is a chemical property associated with planar conjugated cyclic systems like Benzene, and makes use of free delocalized π electrons to improve its high stability and unusual reactivity patterns. In 1930, Hückel published his finding on π systems by using molecular orbital theory, which is referred to as Hückel molecular orbital theory (HMO). Later, in 1931[30], he generalized and extended this theory to benzene and concluded that any conjugated monocyclic polyene that is planar and has $(4n+2)$ π and/or nonbonding electrons, with n = 0, 1, 2, … etc., will exhibit special stability associated with aromaticity. It was not until 1951 that Huckel's $(4n+2)$ π concept was formally clarified by Doering[31]. Although Hückel's aromaticity concept has a great impact in organic chemistry, it has been found not to be valid for several compounds like pyrene, coronene, etc., which have more than three fused cyclic rings. Recently, the concept of aromaticity has been extended to 3D molecules. In 2000 Hirsch *et. al.*[32] gave the $2(N+1)^2$ π electron rule for fullerene aromaticity. According to these authors, this rule should be applicable to all conjugated π systems, including inorganic molecules having symmetrically distributed nuclei over a spherical surface. The aromaticity concept has been further extended to include metals as well through σ and δ bond delocalization, though this is still a hotly debated topic[33].

A classic example of an aromatic molecule is benzene, C_6H_6 which has 6 π electrons (n=1), and a negative electron affinity, namely -1.15 eV[34]. C_5H_5, on the other hand, has 5 π electrons, and needs one more electron to be aromatic. Consequently, the electron affinity of C_5H_5, namely, +1.79 eV[35] is significantly larger than that of C_6H_6. However, it is much less than that of any halogen atom. Thus, it is not immediately apparent if molecules designed by following aromaticity concepts can exhibit superhalogen properties. This is because aromatic molecules are usually characterized by covalent bonding where the electrons are localized along the bonds. In a superhalogen, on the other hand, the electrons should be delocalized over a large phase space so that the electron-electron repulsion associated with the added electron is limited. To form superhalogens, the electron affinity of C_5H_5 should be cultivated towards larger values by further delocalizing the free π electrons. I have explored two possible methods to enact this effect. The first is by replacing the H atoms of C_5H_5 with ligands, and the second is by replacing the C atoms while keeping the $4n$+2 delocalized π electrons unchanged. I also show that the effect of the second method can be expanded by the annulation of more rings to the system, granting more potential substitution sites.

1.4 Induction of superhalogen behavior in organic molecules

In the prior section, we addressed the possibility of forming superhalogens from aromatic molecules, and develop two systematic methods for the enhancement of this behavior in anionic parent molecules. Here we show that Huckel's rule can still be used for the induction of superhalogen behavior in non-anionic parent molecules. This can be achieved by simultaneously replacing the C atoms in the ring with B, Al, or Ga, to make the ring one electron shy of the $4n$+2 electrons needed for aromatic stability, and the H atoms in the ligand with F or CN moieties to enhance the electron affinity of the ring. This can be seen in scheme 1 and 2 for cyclopropenyl

cation and benzene respectively. Note that both molecules are aromatic with *n*=0 in the former and *n*=1 in the latter. In addition, neutral BC_2H_3 is isoelectronic with $C_3H_3^+$ and hence aromatic while B_2CH_3 would require one extra electron to be aromatic. Similarly, BC_5H_6 would also require one electron to be aromatic. Because aromaticity rule will stabilize the negative ions, we hypothesize that their corresponding neutrals should possess large electron affinities. We then explore larger organic ring structures to see how these methods develop electron affinity with a change in molecular size.

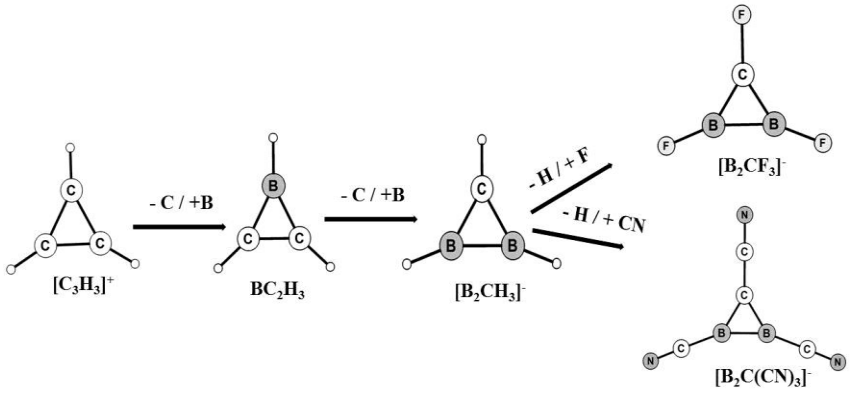

Scheme 1. A schematic representation of the creation of an organic superhalogen from $C_3H_3^+$

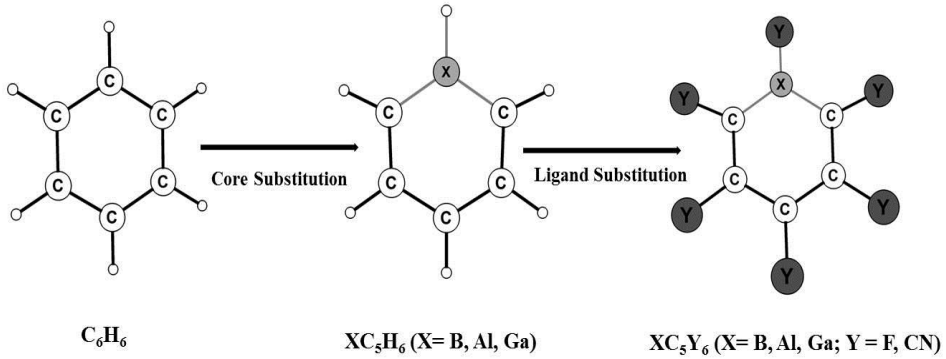

Scheme 2. A schematic representation of the creation of an organic superhalogen from C_6H_6

Theoretical Methods

The total energies and equilibrium geometries of the most stable anions and corresponding neutral molecules were calculated using Density Functional Theory (DFT) and B3LYP hybrid functional [34,35] for exchange-correlation potential with the 6-311+G(d) basis set. Select calculations were done using CCSD *ab initio* methods as well as comparisons to experiment where available were done to confirm the accuracy of the results. Where applicable the SSD basis set was used for transition metals. Frequency analysis was also performed at the same level of theory to ensure that there are no imaginary frequencies and the structure belongs to a minimum in the potential energy surface.

2.1 Schrodinger and Born-Oppenheimer

In 1927 Schrodinger presented his waveform equation that would become the basis for a theoretical approach to the study of the electronic properties of atoms and molecules. According to the time-independent Schrodinger equation

$$\hat{H}\Psi=E\Psi \tag{2.1}$$

the Hamiltonian operator $\hat{H}$ acting on the wave function Ψ will result in the scalar Eigen value E times the wave function. The Hamiltonian operator for a many particle system can be written as

$$\hat{H} = -\frac{\hbar^2}{2m_e}\sum_{i=1}^{N}\nabla_i^2 - \frac{\hbar^2}{2M_A}\sum_{A=1}^{M}\nabla_A^2 - e^2\sum_{i=1}^{N}\sum_{A=1}^{M}\frac{Z_A}{r_{iA}} + e^2\sum_{i=1}^{N}\sum_{j>i}^{N}\frac{1}{r_{ij}} + e^2\sum_{A=1}^{M}\sum_{B>A}^{M}\frac{Z_A Z_B}{r_{AB}} \tag{2.2}$$

where N is the number of electrons, M the number of atoms, Z_A and Z_B are atomic numbers, M_A the mass of the nucleus and m_e the mass of an electron. The indices for the summations are *i* and *j* for electrons and *A* and *B* for nuclei, and $\hbar$ is the Planck's constant divided by 2π. The terms, in

order are; kinetic energy for electron, T; kinetic energy for nucleus, T; electrostatic nuclei-electron interaction, V_{Ne}; electron-electron interaction potential, V_{ee}; and nucleus-nucleus interaction potential. Negative terms are attractive and positive terms are repulsive, consistent with the convention. Solving equation (2.1) for exact solutions of Ψ however has thwarted scientists since the equation was proposed. Large systems of particles are just too complex, and even with modern computers would require too much time to find a solution. Many approximations have been made over the last century that brings us to the density functional theory (DFT) that we use today.

One of the first approximations that was made was to assume that the nuclear kinetic energy is zero (the nuclei are inert) leading to a constant nucleus-nucleus interaction term in eq. (2.2). This is called the Born-Oppenheimer approximation[36], which only holds true when $M_A >> m_e$. This allows us to ignore two terms of eq. (2.2) leaving

$$\hat{H} = -\frac{\hbar^2}{2m_e}\sum_{i=1}^{N}\nabla_i^2 - e^2\sum_{i=1}^{N}\sum_{A=1}^{M}\frac{Z_A}{r_{iA}} + e^2\sum_{i=1}^{N}\sum_{j>i}^{N}\frac{1}{r_{ij}}. \qquad (2.3)$$

While this approximation greatly simplified the calculation, it can only be solved exactly for a one electron system. In order to solve larger systems further approximations will need to be made.

2.2 Hartree Method

In 1928 Hartree proposed a new approximation[37] wherein he suggested that an N electron problem could be treated as N one-electron problems. His new Hamiltonian was

$$\hat{H} = \sum_{i=1}^{N}\left[-\frac{1}{2}\nabla_i^2 - \sum_{A=1}^{M}\frac{Z_A}{r_{iA}} + e^2\sum_{j=1}^{N}\frac{1}{r_{ij}}\right] = \sum_{i=1}^{N}[h(i)]. \qquad (2.4)$$

This leads to a wave function that is a simple linear combination of spin orbital wave functions

$$\Psi^{HP}(x_1, x_2, \ldots x_N) = \chi_1(x_1)\chi_2(x_2)\ldots\chi_N(x_N) \qquad (2.5)$$

where χ_i is the spin orbital of the *i*th electron and x_i its position, known as the Hartree product wave function. Solutions can be found with the Hartree eigenvalue equation

$$h(i)\chi_j(x_i) = \varepsilon_j\chi_j(x_i). \tag{2.6}$$

This leads to the eigenvalue, E, of the Schrodinger equation becoming the sum of the individual spin orbital energies

$$E = \varepsilon_1 + \varepsilon_2 + \cdots + \varepsilon_N. \tag{2.7}$$

While this approximation successfully allows simple solutions of eq. (2.1) it has two major failings. First, the process of interchanging electron coordinates is not anti-symmetric, and second, it does not obey Pauli's Exclusion Principle.

2.3 Hartree-Fock Method

Later in 1928 Fock improved upon Hartree's method with the Hartree-Fock approximation[38]. Fock used an anti-symetric determinant of N one-electron wave functions, known as a Slater determinant[39],

$$\Psi_{SD}(x_1, x_2, \ldots x_N) = \frac{1}{\sqrt{N!}}\begin{vmatrix} \chi_1(x_1) & \chi_2(x_1) & \cdots & \chi_N(x_1) \\ \chi_1(x_2) & \chi_2(x_2) & \cdots & \chi_N(x_2) \\ \vdots & \vdots & \ddots & \vdots \\ \chi_1(x_N) & \chi_1(x_N) & \cdots & \chi_N(x_N) \end{vmatrix}. \tag{2.8}$$

The $\frac{1}{\sqrt{N!}}$ term is a normalization term and the determinant inherently includes the electron-electron repulsive potential. It is anti-symmetric with respect to electron coordinate interchange, and obeys Pauli's Exclusion principle as it becomes zero when two electrons have the same spin orbital. This gives the Hartree-Fock eigenvalue equation

$$f(i)\chi_j(x_i) = \varepsilon_i\chi_j(x_i) \tag{2.9}$$

Where *f(i)* is the Fock operator

$$f(i) = -\frac{1}{2}\nabla_i^2 - \sum_{A=1}^{M}\frac{Z_A}{r_{iA}} + V^{HF}(i) \tag{2.10}$$

Replacing the complicated electron-electron repulsive potential term with the simpler one electron Hartree-Fock potential $V^{HF}(i)$,

$$V^{HF}(i) = \sum_j^N J_i(x_i) - K_j(x_i), \quad (2.11)$$

where J and K are Coulomb and exchange operators. Thus the total energy of the Hartree-Fock approximation can be found to be

$$E_{HF} = \langle \Psi_{SD}|H|\Psi_{SD}\rangle = \sum_{i=1}^N \varepsilon_i - \frac{1}{2}\sum_{i=1}^N \sum_{j=1}^N \left(J_{ij} - K_{ij}\right) = \sum_{i=1}^N \varepsilon_i - \langle \Psi_{SD}|V_{ee}|\Psi_{SD}\rangle, \quad (2.12)$$

where J_{ij} is the Coulomb integral

$$J_{ij} = \langle ii|jj\rangle = \int dx_i dx_j \frac{|\chi_i(x_i)|^2 |\chi_j(x_j)|^2}{r_{ij}} \quad (2.13)$$

And Kij is the exchange integral

$$K_{ij} = \langle ij|ji\rangle = \int dx_i dx_j \frac{\chi_i^*(x_i)\chi_j^*(x_j)\chi_j(x_i)\chi_i(x_j)}{r_{ij}}. \quad (2.14)$$

While the Hartree-Fock approximation is more accurate and fixes many of the problems of the Hartree approximation, due to this Coulomb and exchange terms, it is much more computationally intensive than the Hartree method. The Hartree-Fock method also fails to account for short-range electron-electron correlation due to the use of a single Slater determinant that averages the interactions rather than finding them explicitly. This issue can be resolved by using a linear combination of Slater determinants, a process known as Configuration Interaction method (CI). This however would further increase computation time. Other methods that have developed from Hartree-Fock include Coupled Cluster (CC) and Møller-Plesset perturbation theory (MP). All of these methods underestimate the exact result, so their error is predictable. In addition, they are very computation intensive, being based on HF.

2.4 Density Functional Theory

Density functional theory was proposed as an alternative to the HF derived methods where the electron charge density ρ as given by

$$\rho(\mathrm{r}) = \mathrm{N} \int dx_1 \ldots \int dx_N \Psi^*(x_1, \ldots x_N)\Psi(x_1, \ldots x_N), \text{ for N electrons} \qquad (2.15)$$

is used instead of the wave function to compute the total energy.

2.4.1 Hohenberg-Khon Formulation

It was first proposed in 1964 by Hohenburg and Kohn[40] who claimed that an N-electron system could be reduced from a 3N coordinate problem to a 3 coordinate problem by using functional of the electron density. Using eq. (2.3) and the variational principle the energy can be found by minimizing the functional

$$E(\Psi) = \frac{\langle \Psi | H | \Psi \rangle}{\langle \Psi | \Psi \rangle}. \qquad (2.16)$$

The solution is determined by the number of electrons N and the external potential $V(\vec{r})$ defined as the nucleus-electron interaction term

$$V(\vec{r}_i) = -\sum_{A=1}^{M} \frac{Z_A}{r_{iA}}. \qquad (2.17)$$

The Hohenberg-Khon Formulation claims that the total energy can be determined from the electron density ρ. Instead of using the Hamiltonian we can therefore find the total energy by using

$$E(\rho) = T(\rho) + V_{Ne}(\rho) + V_{ee}(\rho), \qquad (2.18)$$

using terms similar to the Schrodinger Hamiltonian (2.2). The V_{Ne} term can be rewritten as

$$V_{Ne} = \int \rho(\vec{r}) V(\vec{r}) d\vec{r}\,. \qquad (2.19)$$

Now Hohenburg and Kohn use the variational principle to state that if $\rho(\vec{r})d\vec{r} \geq 0$ and $\int \rho(\vec{r})d\vec{r} = N$ are true, then

$$E_g \leq E\big(\rho(r)\big). \qquad (2.20)$$

With an appropriate approximation for the kinetic energy and electron-electron terms the density can now be used to find potentially accurate solutions for the total energy of the system.

2.4.2 Exchange-Correlation

Using the Kohn-Sham equations[41] the potential can be redefined as an effective potential

$$V_{eff} = V_c + V_{xc} - V_{Ne}, \tag{2.21}$$

Where V_c is the classical Coulomb potential, V_{xc} is the exchange-correlation potential and V_{Ne} is the familiar nucleus-electron interaction. It is the exchange-correlation term that provides such difficulty in finding a solution. The exchange-correlation energy which can be related to the potential by

$$V_{xc} = \frac{\partial E_{xc}(\rho)}{\partial \rho(\vec{r})} \tag{2.22}$$

can be approximated as

$$E_{xc}\big(\rho(\vec{r})\big) = E_x(\rho) + E_c(\rho) = \int \rho(\vec{r})\varepsilon_x d\vec{r} + \int \rho(\vec{r})\varepsilon_c d\vec{r}, \tag{2.23}$$

where E_x is the exchange energy found with the slater determinant, and E_c is the correlation energy.

2.4.3 Local Density Approximation

In order to better resolve a solution for the E_{xc} term a new approximation can be made. If we treat the electron density as if it were a homogenous gas, then ρ would be slowly varying with r. We can define the LDA approximation of E_x as

$$E_x = -\frac{3}{4}\left(\frac{3}{\pi}\right)^{1/3} \int \rho(\vec{r})^{4/3} d\vec{r}. \tag{2.24}$$

The corresponding potential is

$$V_x(\rho) = -\left(\frac{3}{\pi}\right)^{1/3} \rho(\vec{r})^{1/3}. \tag{2.25}$$

LDA provides a computationally fast way to approximate the exchange energy. However, it is not accurate for systems where the electron density in inhomogenious.

2.4.4 Generalized Gradient Approximation

The addition of the gradient of ρ to the Local Density Approximation, known as GGA, has the form

$$E_x(\rho) = \int \rho(\vec{r})\varepsilon_x\big(\rho(\vec{r}), \nabla\rho(\vec{r})\big)d\vec{r}. \quad (2.26)$$

GGA functionals can improve over the accuracy of LDA by matching the density values as well as its slope, for a minimal increase in cost. Further improvements added are things like appropriate *r* dependence.

2.5 B3LYP and Hybrid Density Functionals

Hybrid density functionals are functionals that fractionally combine multiple different methods. In these hybrids, there is usually a Hartree-Fock term in addition to one or more DFT terms. Each term is usually added to achieve accuracy in some particular area that HF or the other methods do not accurately provide. B3LYP[42] is one such hybrid functional that combines Hartree-Fock with an LDA Slater determinant, Becke's GGA exchange correction, and Lee, Yang, and Parr's GGA correlation functional. This is represented as

$$E_{xc}^{B3LYP} = E_x^{LDA} + a_0(E_x^{HF} - E_x^{LDA}) + a_x\Delta E_x^{B88} + E_c^{VWN} + a_c(E_c^{LYP} - E_c^{VWN}). \quad (2.27)$$

Here a_0=0.20, a_x=0.72, and a_c=0.81 are determined by fitting the solutions to experimental data.

2.6 Basis Sets

We define the molecular orbitals Ψ_i as a linear combination of one electron orbitals, χ_μ, which we will call basis functions. This can be written as

$$\Psi_i = \sum_{\mu=1}^{N} C_{\mu i}\chi_\mu \quad (2.28)$$

where $C_{\mu i}$ are the molecular expansion coefficients and χ_μ is the μ-th orbital of N atomic orbitals. These functionals are often atomic orbitals themselves. There are two types of orbitals commonly used, Slater Type Orbitals (STO)[43] and Gaussian Type Orbitals (GTO)[44]. STO are exponential decay functions with spherical harmonics that make them computationally expensive so, instead GTO functions are often used. GTO functions take the form

$$\chi(x,y,z) = Nx^{l_x}y^{l_y}z^{l_z}e^{-\zeta r^2} \tag{2.29}$$

separating the function into its radial (ζ) and angular (l_x, l_y, l_z) components. GTO functions are used to replace STO functions and are computationally much faster than STO functions; however, their accuracy breaks down at small r where the GTO has a slope of zero. The computation time can be further reduced through contraction of GTO functions with fixed coefficients,

$$\chi_\mu^{CGF} = \sum_{i=1}^{L} d_{i\mu}\chi_i^{GF}(\zeta_{i\mu}, r). \tag{2.30}$$

Here $d_{i\mu}$ is the contraction coefficients, L is the length of the contraction, and $\zeta_{i\mu}$ are the contraction exponents. The basis set can now be calculated using varying numbers of these contracted orbitals. An example would be the 6-311G basis set. This means that the core orbitals are being represented with 6 GTOs contracted together, while the valence orbital is represented with three s-orbital GTOs, one p-orbital GTO, and one d-orbital GTO. The addition of polarization functions, represented by adding a *, can improve the atomic bonding accuracy; while the addition of diffuse functions, represented by a +, can improve the accuracy of long distance orbitals. The 6-311+G(d) basis set was predominately used for this work.

Results

3.1 Results and discussion of superhalogen behavior by core or ligand substitution in aromatic molecules using C_5H_5

As cyclopentadiene (C_5H_5) is already an aromatic anion it appeared to be a good starting point for the exploration into possible superhalogen behavior. A systematic approach was taken to explore two possible mechanisms independently to verify each of their merits; core substitutions, and ligand substitutions.

3.1.1 Validation of theoretical method

To validate our theoretical method for use on aromatic compounds we compare the results for C_5H_5 and C_6H_6 to experiment. The equilibrium structures, bond lengths, and calculated electron affinities (EA) are given in Fig. 1 and Table 1 alongside their experimental values. The C-C bond lengths are 1.37, 1.44, and 1.48 Å for C_5H_5 and 1.39 Å for C_6H_6. The C-H bond lengths of C_5H_5 and C_6H_6 are 1.08 Å and 1.09 Å, respectively. These agree well with corresponding experimental values of C-C bonds, namely, 1.34, 1.46, and 1.54 Å and C-H bond,1.08 Å of C_5H_5, and C-C bond, 1.40 Å, and C-H bond,1.09 Å of C_6H_6. Similarly, the calculated EA of benzene (C_6H_6), which is aromatic, is -1.33 eV and is in good agreement with the experimental value of -1.15 eV. However, the fit between the experiment and theory for the negative EAs may be coincidental because of the limits of the computational model in characterizing species with unbound electrons. We have recalculated the EA of benzene at the

CCSD level of theory and found it to be -1.83 eV. It is expected that C_5H_5 which needs one extra electron to be aromatic would have a larger electron affinity than that of C_6H_6. Although this is indeed the case and the calculated EA of C_5H_5 is +1.72 eV (compared to experimental value of

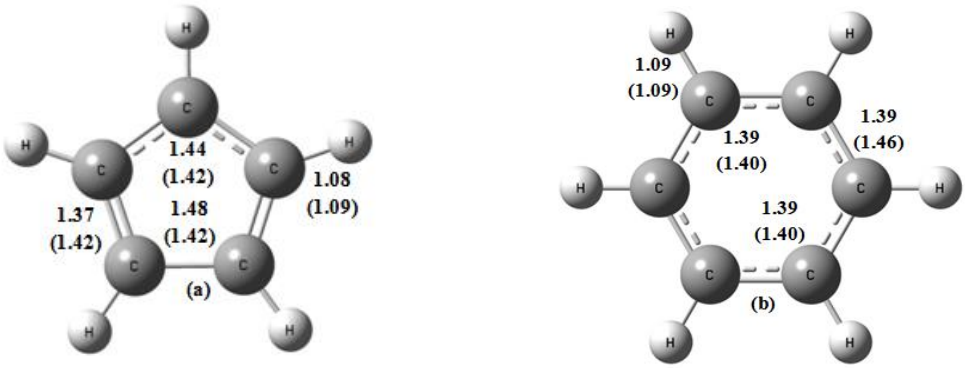

Fig. 1 Equilibrium geometries of C_5H_5 and C_6H_6. The bond lengths are given in Å. The bond lengths in brackets are those of the anion.

+1.79 eV), it is much smaller than that of a halogen atom. At the CCSD level of theory the EA of C_5H_5 is +1.36 eV. Thus, the DFT/B3LYP level of theory overestimates the electron affinity compared to CCSD level of theory. The question then is: can molecules, using aromaticity rules, be designed such that their EAs are larger than those of halogen atoms? To examine this possibility a systematic approach was adopted.

3.1.2 Ligand substitution: C_nX_n (X= F, CF_3, NCO, CN, BO_2; n=5, 6)

First, we try to design aromatic superhalogens by ligand substitution in C_5H_5, keeping the aromatic core intact. To do so we replace H in C_5H_5 by different ligands such as F, CF_3, NCO, CN, and BO_2 since these are far more electronegative than H. For example, the electron affinities of F, CF_3, NCO, CN, BO_2 are, respectively, 3.40, 1.89, 3.58, 4.07 and 4.35 eV while that of H is only 0.75 eV. The equilibrium geometries of C_5X_5 (X= F, CF_3, NCO, CN, BO_2) molecules are given in Fig 2. Note that in the case of $C_5(CN)_5$ and $C_5(NCO)_5$, the C atom on the ring can either bind to the C or N atom of CN and N or O atom of NCO, respectively. In addition, in the case

$C_5(BO_2)_5$ the ligands can dimerize and bind to the C atoms in the ring. Only the lowest energy configurations are given in Fig. 2. Similar calculations were repeated for the benzene, C_6H_6, where the H atoms were replaced by F, CN, BO_2 ligands. The equilibrium geometries of the C_6X_6 (X= F, CN, BO_2) molecules along with their electron affinities can be found later in section 3.4.

The CF bond length in C_5F_5 is elongated over that of CH bond in C_5H_5 by 0.24 Å. In other molecules in Fig. 2 the bond linking the C atom in the ring to the nearest atom in the ligand varies between 1.37 Å to 1.52 Å. These bonds are stretched further in the corresponding anions. The C-C bonds in the ring, however, are not affected significantly by the different ligands. The ground state geometry of $C_5(NCO)_5$ is marked by the C atom in the ring binding to the N atom in the ligand and is 7.80 eV lower than its isomer where the C atom in the ring binds to the O atom in the ligand. In the lowest energy structure of $C_5(CN)_5$, the C atoms in the ring bind to the C atoms in the ligands while its isomer with C binding to N lies 5.40 eV above in energy. The lowest energy structure of $C_5(BO_2)_5$ departs from the other structures in Fig. 2. Here two of the BO_2 moieties dimerize and bind to four of the carbon atoms in the ring while the fifth carbon atom is bound to the remaining BO_2 ligand. The isomer where each of the C atoms is bound to a single BO_2 unit lays 2.51 eV above the lowest energy structure. This is because the BO_2 moieties gain 1.70 eV of energy by forming a dimer. This, as we will see in the following, has important effect on the expected superhalogen property of the $C_5(BO_2)_5$ molecule.

The EAs of C_6F_6 and C_5F_5 are calculated to be 0.75 eV and 2.68 eV, respectively. Although this is a considerable improvement over the values in C_6H_6 and C_5H_5, replacing H by F does not lead to a superhalogen. However, the situation changes with different ligands. The EA of $C_5(CN)_5$ is 5.59 eV, making it a superhalogen. To confirm the accuracy of our method we also calculated the electron affinity of $C_5(CN)_5$ at the CCSD level of theory. The corresponding value, namely 5.30 eV, is 0.3 eV less than that of the value at the CCSD level of theory. This is consistent with previous results[45] that the electron affinities calculated at the DFT level of theory is usually accurate within about 0.2 eV. The EA of $C_5(NCO)_5$ and $C_5(BO_2)_5$ are 3.28, and 3.45 eV, respectively. Although these are significantly enhanced over that of C_5F_5, $C_5(NCO)_5$ and $C_5(BO_2)_5$ do not belong to the superhalogen category. The reason for $C_5(BO_2)_5$ not becoming a

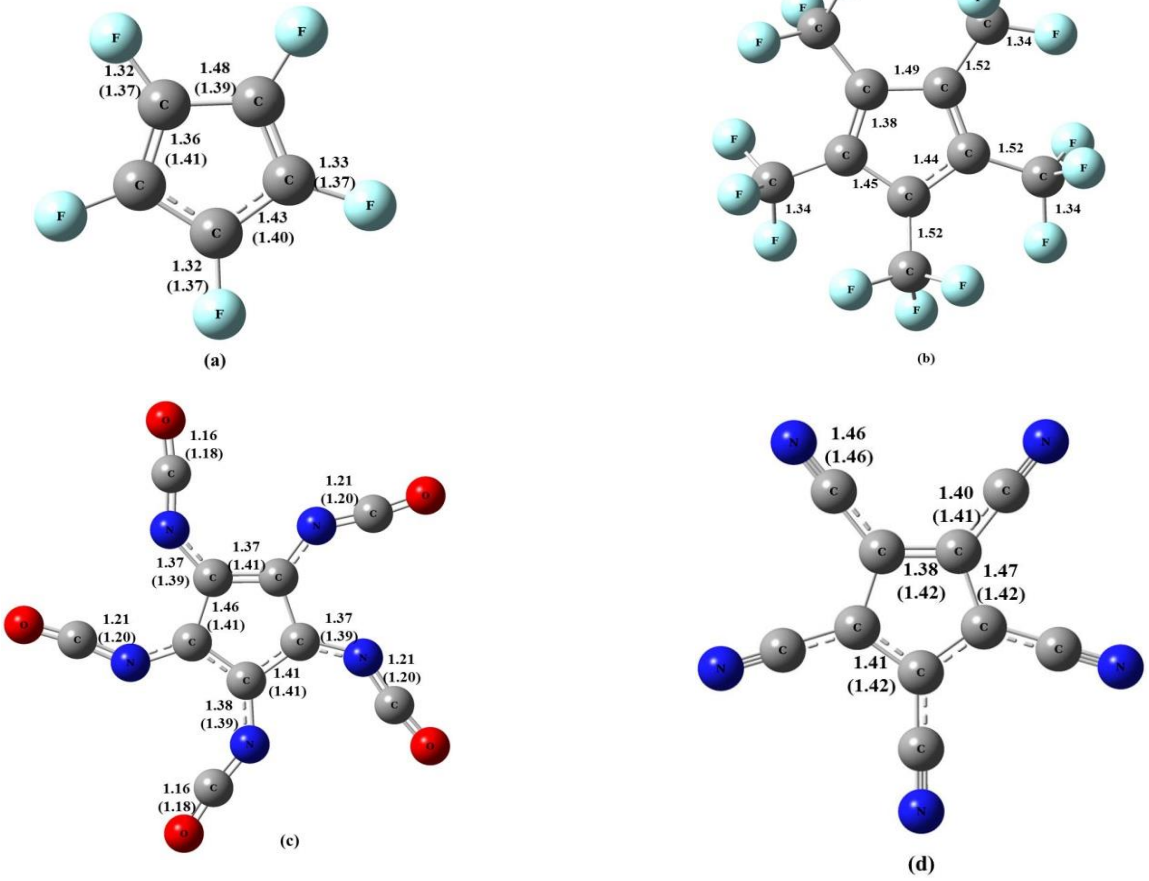

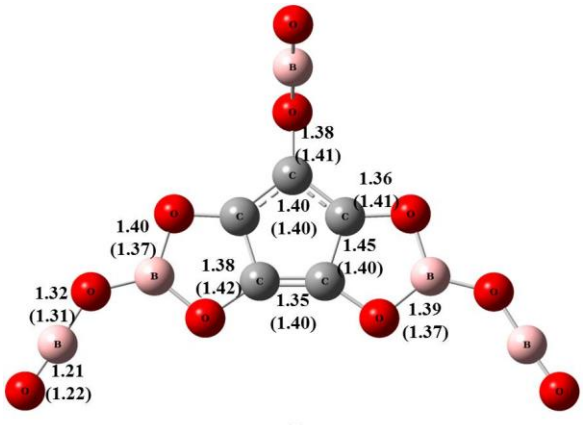

Fig. 2 Equilibrium geometries of C_5X_5 (X= F, CF_3, NCO, CN, BO_2). The bond lengths are given in Å. The bond lengths in brackets are those of the anions.

superhalogen is due to the preference of BO_2 moieties to dimerize. Had that not been the case and each of the C atoms in the ring would have bound to individual BO_2 moieties, the electron affinity of such a complex would have been 4.25 eV, making it a superhalogen. The probable reason for C_5F_5 and $C_5(NCO)_5$ not becoming a superhalogen is that the π donating nature of F and NCO works against it. The same conclusion also holds for BO_2. CN as a ligand works better for making a superhalogen because of its dual nature. CN is not only a strong electron withdrawing group but also has a high electron affinity. So it is clear that electron withdrawing effect of the ligand drives the formation of superhalogen compounds.

To check this idea further we considered CF_3 ligand which belongs to an electron withdrawing group having low EA value (1.89 eV). To calculate EA of $C_5(CF_3)_5$ molecules we tried to optimize both the neutral and the anion geometry. While we were successful in optimizing the neutral geometry, the optimization of its anion geometry led to problems. The imaginary negative frequencies were associated with the rotation of the CF_3 unit in $C_5(CF_3)_5$. Therefore, we calculated the vertical attachment energy (VAE) which is the energy gained by attaching an electron to the neutral structure without optimizing its geometry. In this sense the VAE is lower bound to the EA. The calculated VAE value of $C_5(CF_3)_5$, namely 4.58 eV,

suggests that $C_5(CF_3)_5$ indeed is a superhalogen molecule, owing to the electron withdrawing property of CF_3 ligand. In fact we compared the VAE of $C_5(CF_3)_5$ with that of $C_5(CN)_5$. We found that the VAE of $C_5(CN)_5$ is 5.46 eV which is smaller than its EA, namely 5.59 eV.

3.1.3 Core substitution: $C_{n-m}H_{n-m}N_m$ (n=5, 6; m=0-3)

Now for the second possibility, core substitution, through the replacement of CH groups with N atoms. Note that this replacement leaves the total number of valence electrons unchanged as both CH and N are isoelectronic. Hence, aromatic properties would not be affected by this substitution. However, the electron affinities of CH and N are, respectively, 0.077 eV and 0.073 eV[46]. On this basis one might expect that successive replacement of CH with N in C_6H_6 and C_5H_5 may not lead to moieties with larger electron affinities. However, a previous experimental study had shown

$C_{5-m}H_{5-m}N_m$ **$C_{6-m}H_{6-m}N_m$**

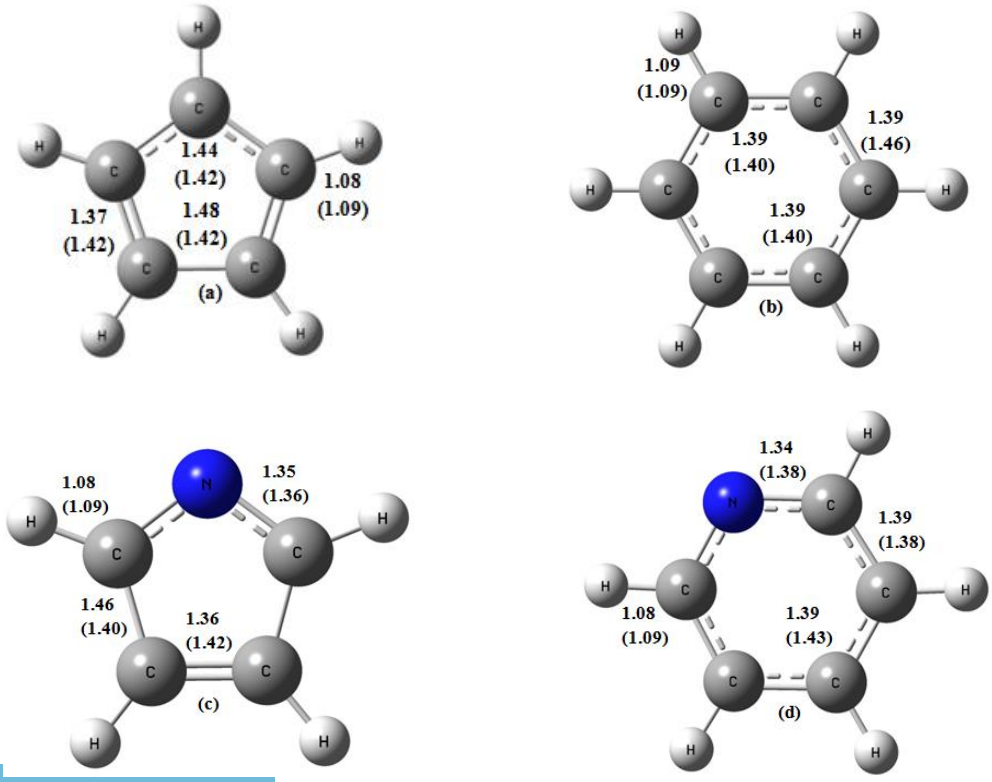

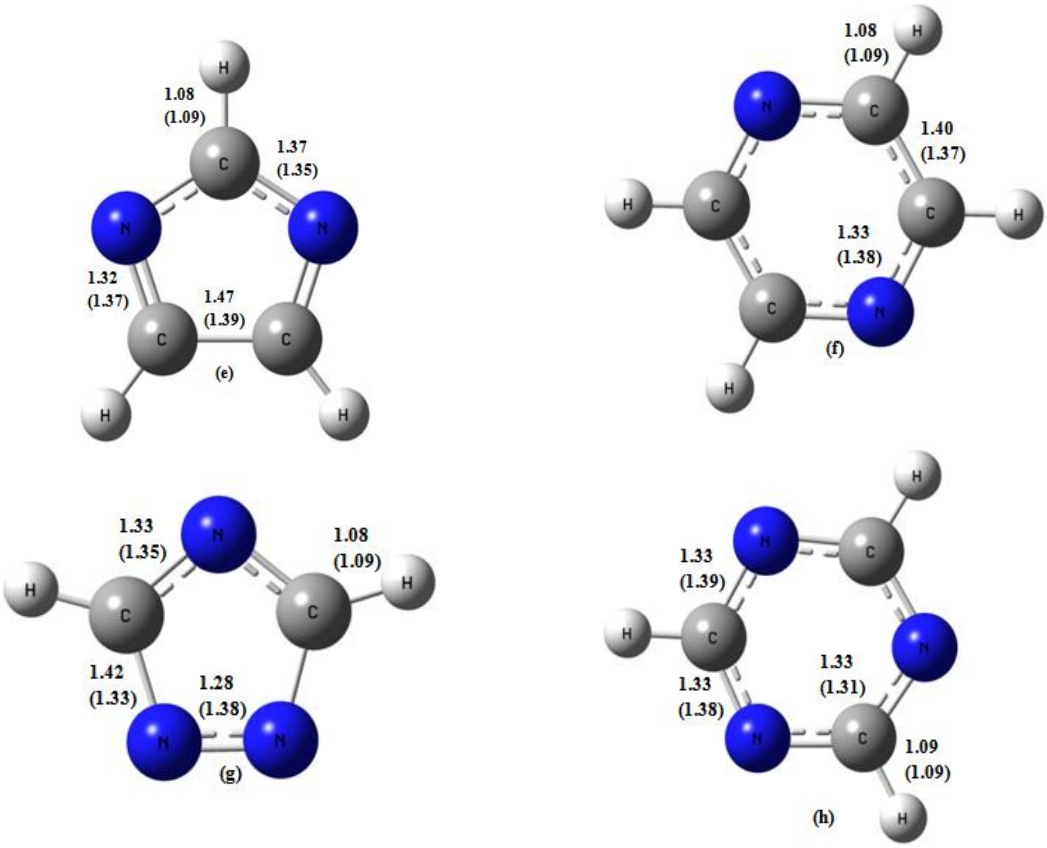

Fig. 3 Equilibrium geometries of $C_{n-m}H_{n-m}N_m$ (n=5, 6, m=0-3). The bond lengths are given in Å. The bond lengths in brackets are those of the anion.

that the EA of C_5H_5N (pyridine) is -0.62 eV[34] which is much more positive than the EA of isoelectronic C_6H_6, namely, -1.15 eV. To study the effect of successive replacement of CH groups with N atoms we calculated the structure and total energies of $C_{n-m}H_{n-m}N_m$ (n=5, 6; m=1-3) systematically. In Fig. 3 we present the geometries of these molecules. The corresponding EAs are given in Table 1. The calculated EA of pyridine is -0.74 eV which is in good agreement with the experimental value (-0.62 eV) given in Table 1. We note that the EA increases steadily with increasing number of N substitutions. The calculated EA of pyrazine and s-triazine where the N atoms are substituted at the 1, 4 and 1, 3, 5 sites are -0.04 eV and +0.008, respectively. These also agree well (within the accuracy of the DFT methods) with the corresponding experimental values of +0.065 eV and +0.124 eV[34]. We note that none of these molecules mimic halogens, let alone superhalogens. No experimental values of the EA of $C_{5-m}H_{5-m}N_m$ (m > 0)

were found. However, our computed values show that the EAs continue to increase and reach a value of 3.46 eV for $C_2H_2N_3$, making this molecule a pseudo-halogen. This shows that it is unlikely that modification of the core of C_5H_5 alone can render it with superhalogen properties.

Table 2: Electron Affinities (in eV) of $C_{n-m}H_{n-m}N_m$ (n=5, 6, m=0-3)

	$C_{6-m}H_{6-m}N_m$		$C_{5-m}H_{5-m}N_m$	
m, # N replaced	**Theory**	**Experiment**	**Theory**	**Experiment**
0	-1.33(-1.83)*	-1.15	1.73(1.36)*	1.79
1	-0.74	-0.62	2.08	
2	-0.04	0.065	2.58	
3	0.008	0.124	3.46	

* Value given in parenthesis is the data calculated at CCSD/6-311+G(d)

3.1.4 Core substitution with ring annulation: $C_{13-m}H_{9-m}N_m$ (m=0-3, 9)

To search for other routes that can enable organic molecules to have electron affinities higher than that of $C_2H_2N_3$, we drew inspiration from an earlier work by Gonzales *e.t al.*[47] where the authors studied a series of molecules by fusing a five-membered ring (C_5H_6) with increasing numbers of six-membered rings. Note that there are two ways to fuse these rings; the five-membered ring may be fused either at the end of the chain or in the middle. The first arrangement with one five-membered ring sandwiched between two six-membered rings is known as fluorene while the latter with a five-membered ring attached at the end of the two fused six-membered rings yields a molecule known as benzo[*f*]indene. At the B3LYP level of theory with the 6-311++G* basis sets the calculated EAs[47] of the radicals formed by cleavage of

a C-H bond in the 5-membered ring, i.e., cyclopentadienyl (C_5H_6), indenyl (C_9H_8), and fluorenyl ($C_{13}H_{10}$), were found to be -0.66 eV, -0.55 eV, and -0.27 eV, respectively. Note that the parent molecules have saturated carbons in the 5-membered ring and the C-H cleavage at this carbon is needed to give a fully delocalized π-system. Addition of an electron gives a closed-shell anion with an aromatic electron count in the π-system. The trend clearly shows that by increasing the length of the organic framework the electron affinity can steadily increase. This is consistent with the expectation that electron affinities tend to increase as electrons are more delocalized.

Since replacement of CH with N or H with F as well as incorporating benzoannulated cyclopentadienyl units tend to increase electron affinities, we considered the base structure of the fluorenyl radical ($C_{13}H_9$) as a starting point in our search for aromatic superhalogens. Note that $C_{13}H_9^-$ satisfies the aromaticity rules. Similar to what was done for C_nH_n (n=5, 6) we first replaced H with F. This did not increase EAs significantly. These results are given later in section 3.4. Next up to three CH groups were replaced with three N atoms successively by considering both the fluorene and benz[*f*]indene frameworks.

3.1.4.1 Equilibrium Geometries of the negative ions

In photoelectron spectroscopy experiments (PES) the starting point is the negative ion. Therefore, we first present the optimized geometries of the most stable isomer of the anionic $C_{13-m}H_{9-m}N_m$ (m=0-3) molecules in Fig. 4(a-e). The ground state of the anionic $C_{13}H_9$ molecule in Fig. 4(a) has the five-membered ring sandwiched between the two six-membered rings (fluorene structure). The higher energy isomer has the benz[*f*]indene structure and lies only 0.29 eV above the ground state (see Fig. 5(a)). These results agree with earlier studies of Gonzales *et. al.*[47].

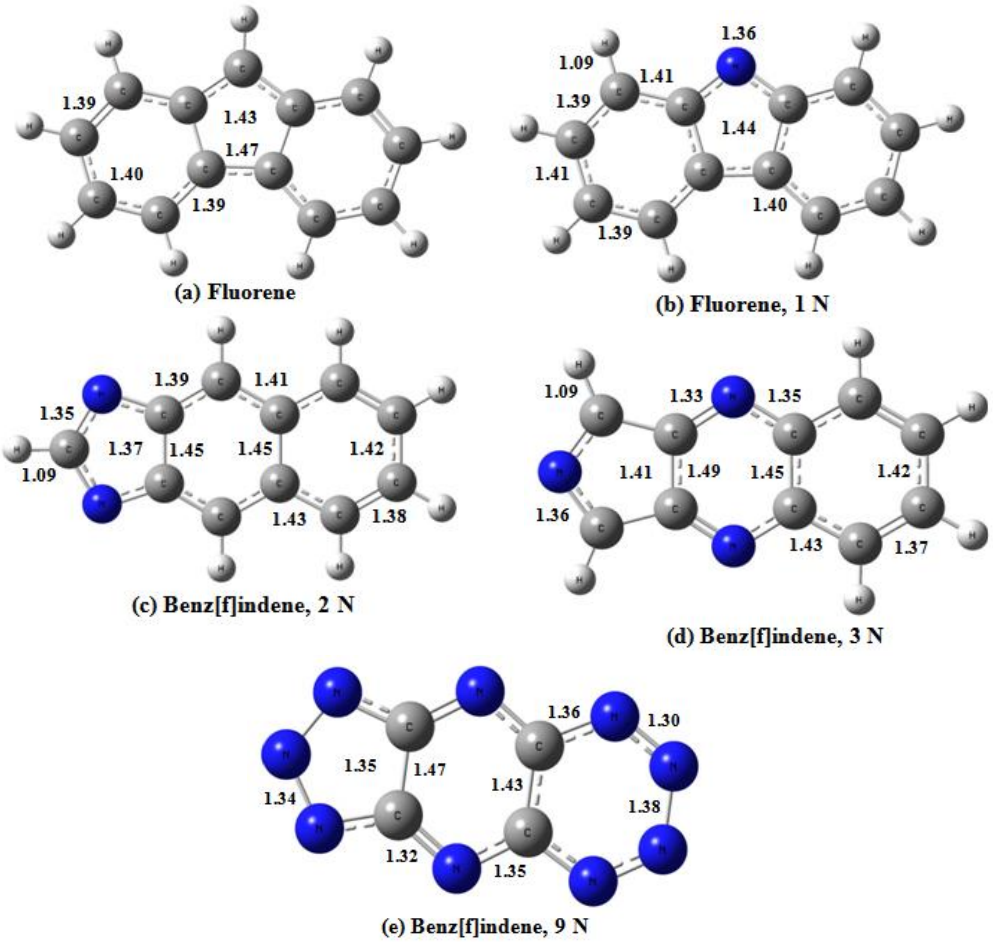

Fig. 4: Equilibrium geometries of anionic $C_{13-m}H_{9-m}N_m$ (m=0-3, 9) molecules. Bond lengths are in Å.

When one of the CH groups is replaced by an N atom, the preferred geometry of the anionic $C_{12}H_8N$ continues to have the fluorene structure. The N atom occupies the 9-position (Fig. 4(b)). The bond lengths are symmetric from left to right and vary from 1.39 Å to 1.41 Å. The nitrogen bonds shorten to 1.36 Å. In Fig. 5(b) we show the geometry of the next higher energy isomer lying 0.65 eV above the ground state. It has the benz[*f*]indene structure where the N atom occupies the end site of the five-membered ring.

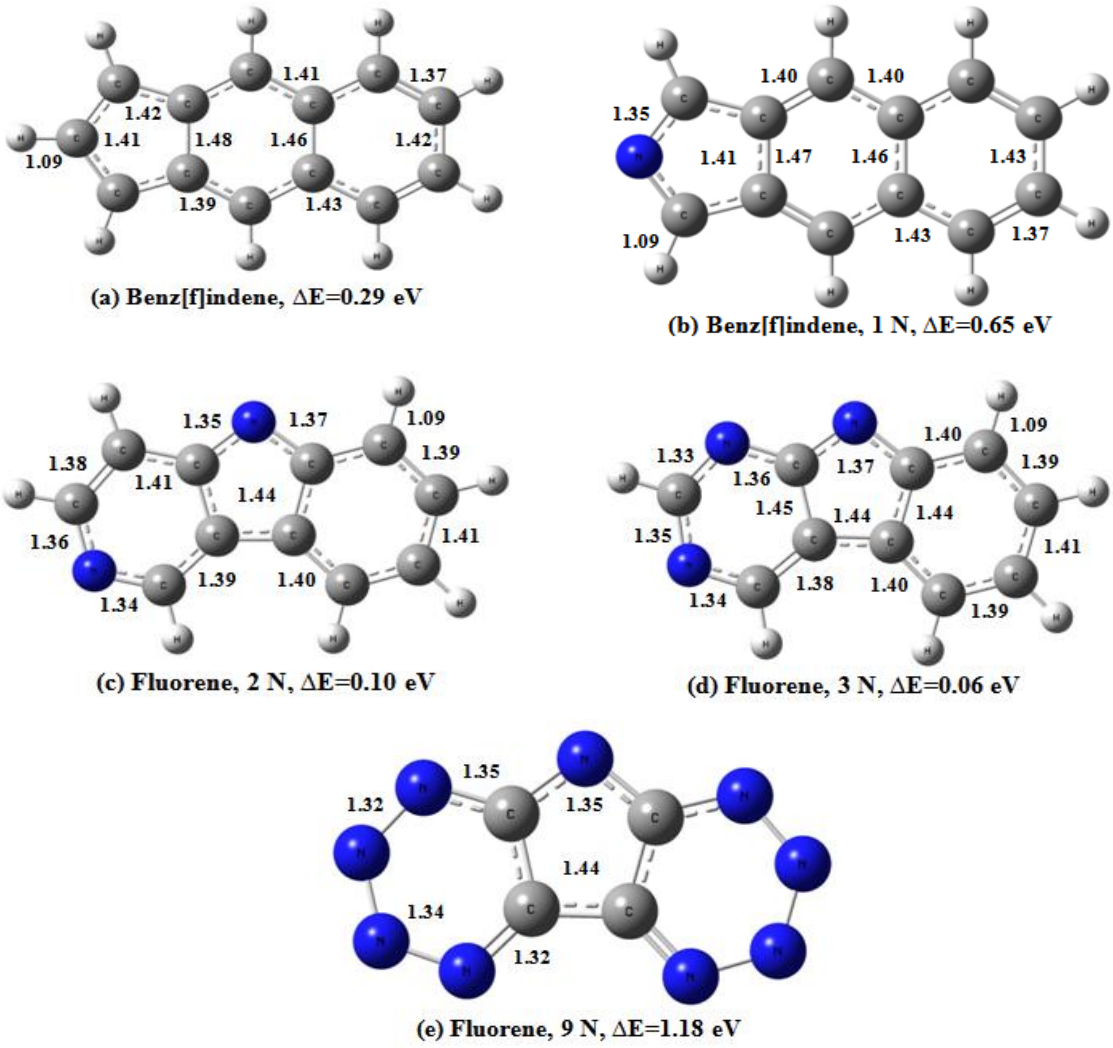

Fig. 5: Geometries of next higher energy isomers of anionic $C_{13-m}H_{9-m}N_m$ (m=0-3, 9) molecules. Bond lengths are in Å.

Next we discuss the replacement of two CH groups with two N atoms. All possible sites for the N atoms were tried and the preferred structure of the anionic $C_{11}H_7N_2$ molecule is shown in Fig. 4(c). Unlike the $C_{12}H_8N$ structure, the $C_{11}H_7N_2$ anion has the benz[*f*]indene structure with the N atoms occupying next nearest neighbor sites in the five-membered ring. The four nitrogen bonds range in length from 1.34 Å to 1.37 Å, while the benzene ring's bond lengths stay unchanged. The bonds in the five-membered ring also increase, but only slightly to 1.45 Å. Preferred locations of N atoms in the next higher energy isomer given in Fig. 5(c) are different as is the

structure. The anion assumes the fluorene structure and lays 0.1 eV above the ground state. One N atom occupies the 9-position of fluorene while the second occupies the farthest site in the six-membered ring. We note that even though the two isomers are rather close in energy, a substantial energy barrier will be involved in going from the benz[*f*]indene structure to the fluorine structure. Thus, if the molecules are born as anions, it is the VDE of the benz[*f*]indene structure that the PES experiment will measure.

The preferred geometry of the $C_{10}H_6N_3$ anion is shown in Fig. 4(d). It has again the benz[*f*]indene structure with one of the N atom occupying the apex site of the five-membered ring while the other two occupy opposite sites in the central six-membered ring. The only change that occurs in the bonds is that those adjacent to the third nitrogen shorten to 1.33 Å and 1.36 Å leaving the far side of the structure unaffected. The corresponding higher energy isomer is shown in Fig. 5(d). Here the anion has the fluorene geometry lying only 0.06 eV above the ground state. One N atom occupies the apex site of the five-membered ring while the other two occupy next nearest neighbor sites of the six-membered ring. Both isomers can be considered to be energetically degenerate and in a PES experiment both are likely to be present. As a general remark, we note that by the time two CH groups are replaced by two N atoms, the anions assume benz[*f*]indene form.

For reasons that will be clear in the following sub-section we next considered structures where all the CH groups were replaced with N atoms. The preferred geometry of the C_4N_9 anion is shown in Fig. 4(e). It assumes the benz[*f*]indene structure. The corresponding geometry of the higher energy isomer is given in Fig. 5(e). The fluorene structure of the anion is 1.18 eV less stable than the benz[*f*]indene form.

3.1.4.2 Vertical Detachment Energies

The vertical detachment energies (VDE) of $C_{13-m}H_{9-m}N_m$ (m=0-3, 9) molecules are given in Table 2. The VDE of $C_{13}H_9$ is 1.82 eV. It increases by 0.69 eV when only one CH group is replaced by N, namely the VDE of $C_{12}H_8N$ is 2.51 eV. The VDEs of $C_{11}H_7N_2$ and $C_{10}H_6N_3$ are, respectively, 2.94 eV and 3.57 eV. Although the VDEs increase with the successive replacement of CH groups with N atoms, $C_{11}H_7N_2$ and $C_{10}H_6N_3$ are still far from being a superhalogen. At best, $C_{10}H_6N_3$ can be termed as a pseudohalogen as its electron affinity approaches that of Cl. Note that while none of these molecules qualify as superhalogens, the VDEs steadily rise with the replacement of CH groups with isoelectronic N. Consequently, we tried the ultimate structure where all the CH groups are replaced with N atoms. This leads to the molecule with formula C_4N_9 which has a VDE of 5.28 eV, clearly making it a superhalogen.

3.1.4.3 Ground State Geometries of Neutral Molecules, Electron Affinities and Adiabatic Detachment Energies

In a PES experiment the first peak in the spectrum corresponds to the vertical detachment energy (VDE) which signifies the least energy needed to remove the extra electron from the anion without changing its structure.

Table 2: VDE, EA, and ADE (in eV) of $C_{13-m}H_{9-m}N_m$ for m=0-3, 9.

# CH groups replaced by N	VDE	EA	ADE
0	1.82	1.74	1.74
1	2.51	2.41	2.43
2	2.94	2.77	2.88

3	3.57	3.10	3.32
9	5.28	4.58	4.58

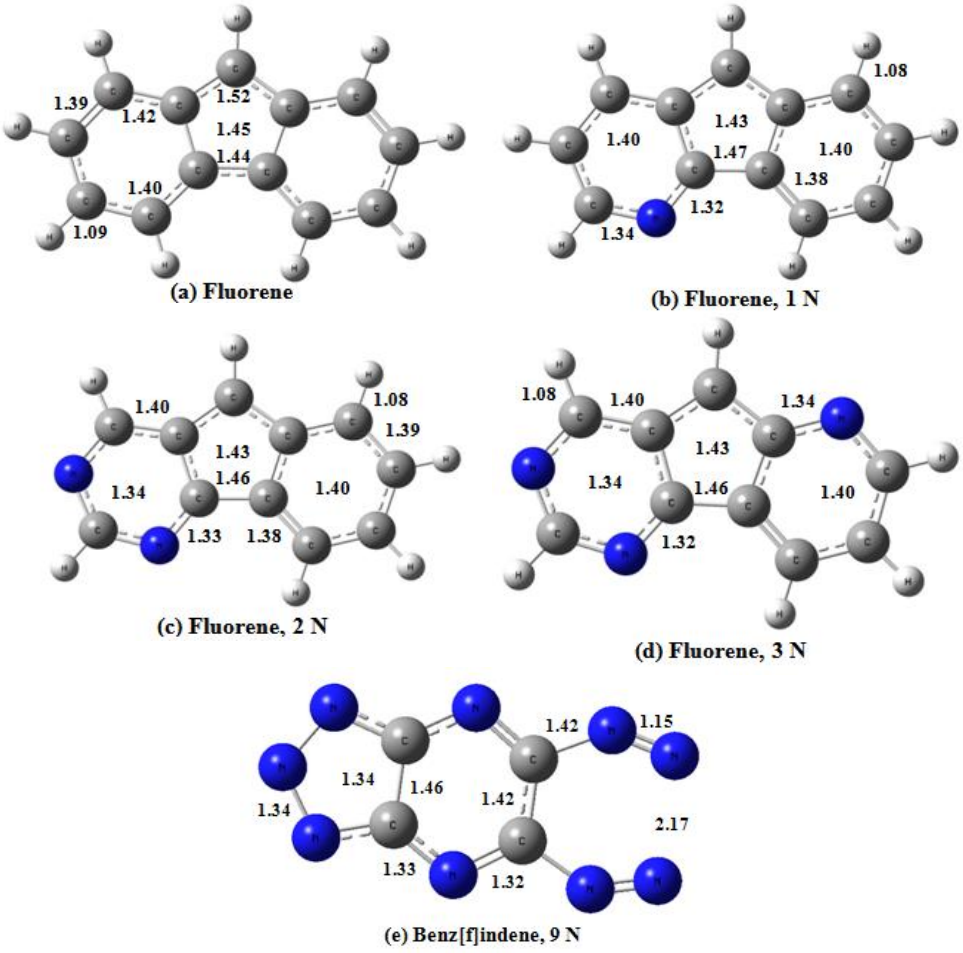

Fig. 6: Ground state geometries of neutral $C_{13-m}H_{9-m}N_m$ (m=0-3, 9) molecules. Bond lengths are in Å.

However, following the electron detachment the neutral cluster will relax. In most cases the neutral cluster will reach its ground state. However, if the geometries of the ground states of the anion and its corresponding neutral are very different and are separated by a large energy barrier, the neutral cluster, following electron detachment, will relax to its nearest potential energy minimum. The difference between the total energy of the anion and its structurally similar

neutral is known as adiabatic detachment energy (ADE) while that between the ground states of the anion and its neutral is referred to as the electron affinity (EA). In most cases the ADE and EA values are rather close, although exceptions do exist. To see how different are the lowest energy geometries of the neutral $C_{13-m}H_{9-m}N_m$ (m=0-3, 9) molecules from their anions, we have optimized their structures. The results are presented in Fig. 6(a-e). The geometries of the next higher energy isomers are given in Fig. 7. The ground state of neutral $C_{13}H_9$ has the fluorene structure, same as that of the anion. The higher energy isomer with the benz[*f*]indene structure lies 0.23 eV above the fluorene structure. Although neutral $C_{12}H_8N$ has the same fluorene structure as its anion, the placement of the N atom is different. In the neutral structure, nitrogen occupies the base of the benzene ring adjacent to the five-membered ring. As in the anion, the nitrogen bonds are shortened to 1.34 and 1.32 Å. The rest of the benzene bonds are 1.40 Å, with the exception of the bonds symmetric with the nitrogen bonds which are 1.38 Å. The bonds of the five-membered ring are 1.43 Å for four sides and the base is 1.47 Å. The geometries of neutral $C_{11}H_7N_2$ and $C_{10}H_6N_3$ have fluorene structure while their anions have the benz[*f*]indene structure.

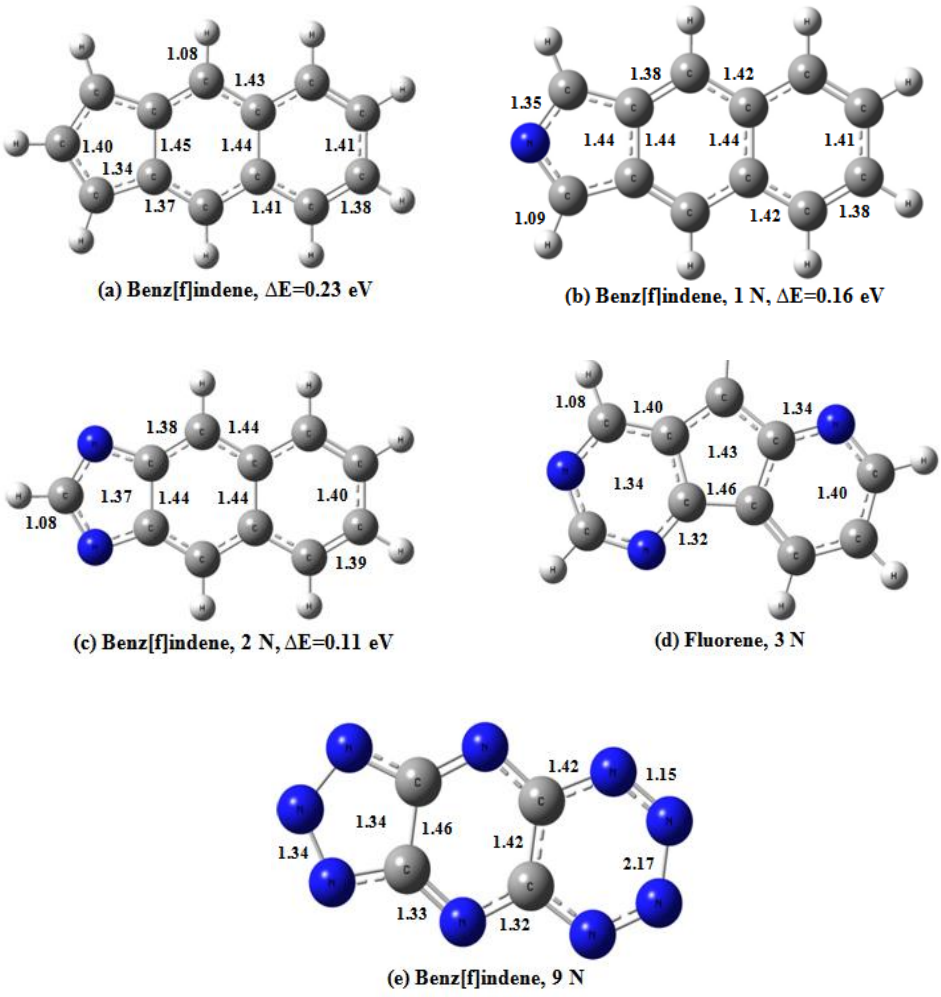

Fig. 7: Geometries of next higher energy isomers of neutral $C_{13-m}H_{9-m}N_m$ (m=0-3, 9) molecules. Bond lengths are in Å.

The nitrogen atoms occupy next nearest neighbor sites of a six-membered ring. In $C_{10}H_6N_3$ the third nitrogen prefers the second six-membered ring and occupies the CH site closest to the five-membered ring. Here, the only change to the bond lengths is that the bonds associated with the third nitrogen atom reduce to 1.34 Å. The ground state of neutral C_4N_9 has the same benz[*f*]indene structure as its anion. The EAs and ADEs of $C_{13-m}H_{9-m}$ N_m (m=0-3, 9) molecules are listed in Table 2. Note that in spite of the large differences in the geometries of the anion and neutral, the EA values are not very different from those of the VDEs. This is because changing

the location of N atoms does not affect the energies significantly, although they will face significant energy barriers to do so.

3.1.5 Thermal Stability

We note from the above that C_4N_9 is a superhalogen and is vibrationally stable since all frequencies are positive. But, is it thermally stable? To examine its thermodynamic stability we calculated the dissociation energies of neutral C_4N_9 against possible fragmentation pathways. First, we considered fragmentation into C_4N_7+N_2 and C_4N_5+2N_2. The first channel is endothermic by 1.11 eV while the second one is exothermic by 0.47 eV [see Fig. 8(a)]. The fragmentation of C_4N_9 where the N_2 molecule is removed from the five-membered ring is endothermic by 0.74 eV. To see if a superhalogen can be created that is *thermally stable* we considered $C_6N_7H_2$ where the two N atoms in the C_4N_9 molecule are replaced by two CH groups [see Fig. 8(b)]. This structure is *stable* against the fragmentation pathway where N_2 breaks away from the five-membered ring. And, most importantly, it is a superhalogen with vertical detachment energy of 4.66 eV.

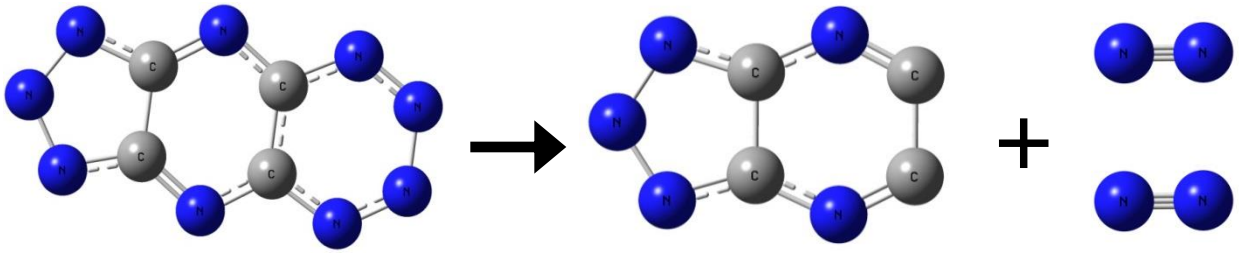

Fig. 8(a): Fragmentation reaction pathway

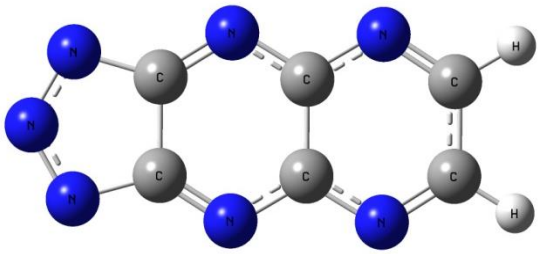

Fig. 8(b): $C_6N_7H_2$, thermally stable

3.1.6 Beyond tricyclic poly aromatic hydrocarbons (PAH)

We note that Gonzales *et. al.*[47] had shown that by increasing the number of benzene rings the EA of a molecule could be increased. To see if replacement of CH groups with N and further addition of benzene rings can continue to yield moieties with higher electron affinities, we studied the structure and properties by successively adding up to six benzene rings to a five-membered ring. The corresponding geometries of the anions are given in Fig. 9. The resulting EAs and VDEs are illustrated in Fig. 10, and the values are presented in Table 3. Note that the EAs and VDEs continue to rise and reach a value of 5.12 and 5.33 eV, respectively. From the NBO charge distributions we found the additional charge to be mostly associated with the

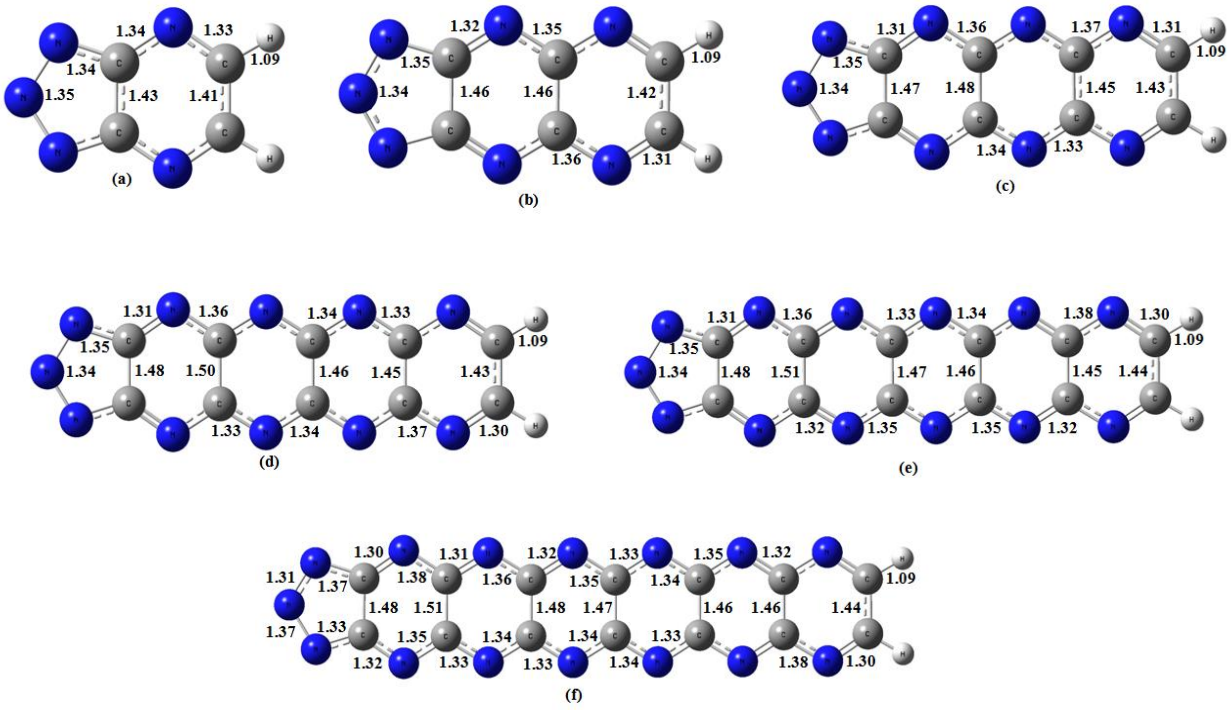

Fig. 9: Ground state geometries of anionic PAH molecules. Bond lengths are in Å.

nitrogen located at sites in the five-membered ring. The nitrogen atoms located in the six-

membered rings have a diminishing charge with increasing distance from the five-membered ring.

Table 3: Electron Affinities (EA) and Vertical Detachment Energies (VDE) of poly aromatic hydrocarbons

	EA	VDE
1 Benzene	4.03 eV	4.36 eV
2 Benzene	4.36 eV	4.66 eV
3 Benzene	4.62 eV	4.95 eV
4 Benzene	4.82 eV	5.09 eV
5 Benzene	4.98 eV	5.23 eV
6 Benzene	5.12 eV	5.33 eV

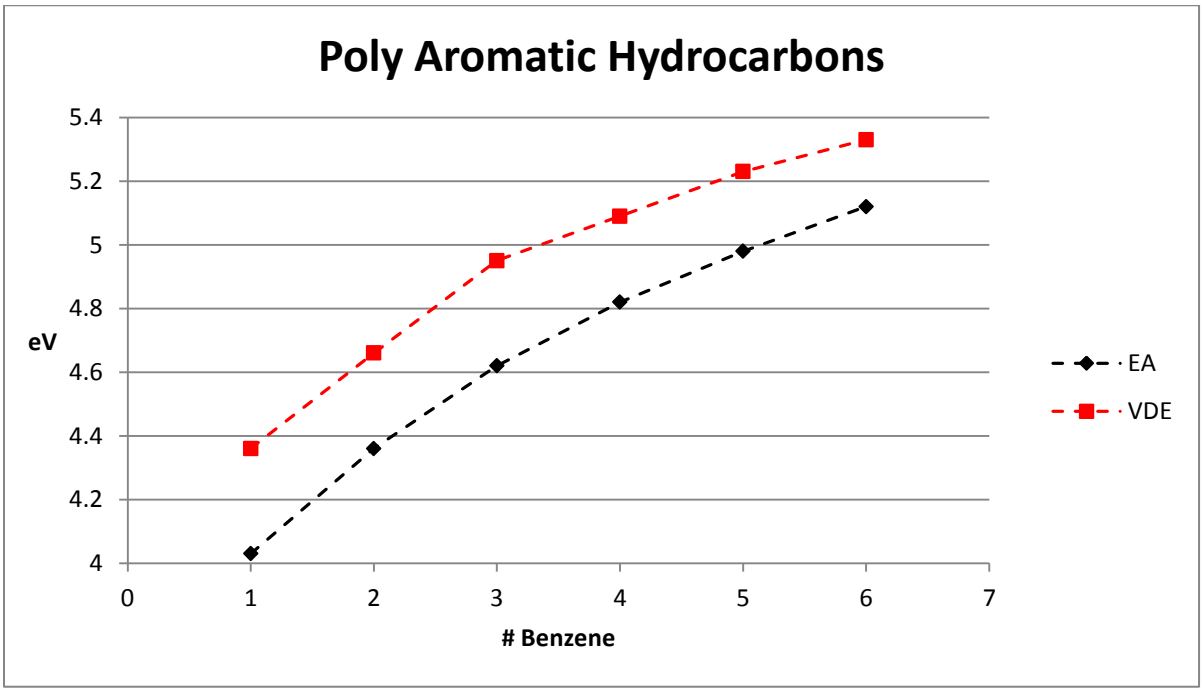

Fig. 10: EA and VDE of larger nitrogen replaced PAH molecules

3.1.7 Aromaticity

Aromaticity can be considered as an indicator of cyclic delocalization of electrons moving freely around the ring. There are different methods available in the literature to predict the aromaticity of a molecule. Some of these are diamagnetic susceptibility exaltation, electron localization function (ELF), harmonic oscillator model of aromaticity (HOMA), nucleus-independent chemical shift (NICS), etc. Here we have adopted the NICS method developed by Schleyer and coworkers[29,48,49]. NICS is defined as the *negative* of the absolute magnetic shielding computed at the un-weighted geometric center of an aromatic or anti-aromatic ring [NICS(0)], or 1A° above the ring [NICS(1)]. Significantly negative NICS values indicate the presence of a diatropic ring current and, therefore, aromaticity in the system. To confirm the aromaticity of these molecules we calculated the chemical shift[48,49] at the center of the ring and 1 Å above it for C_5X_5 (X= F, NCO, CN, BO_2) as well as the first four molecules in Fig. 9. We also studied how these change with ligand and size. We recognize that the increase in the NICS value above the ring is due to the existence of π electrons. Fig. 11 shows the structures with their calculated NICS values (in ppm). The NICS value 1 Å above the plane is listed first, and the NICS value at the center is listed second in *italics*.

We have found that for all the cases of C_5X_5 (X= F, NCO, CN, BO_2) (see Fig. 11(a)) the molecules are aromatic due to their negative NICS values. In fact the aromaticity increases in comparison to that of the cyclopentadienyl anion. We also found that with an increase in aromaticity, the EA also increases. For the second sets of molecule (Fig 11 (b)) the cyclopentadienyl anion starts out with the highest NICS value for both in the plane and above it. As more benzene rings are added, the aromaticity in the ring decreases. The NICS value of the benzene ring at the end of the chain (marked "1") also decreases with increasing chain length.

However, the aromatcity of the inner benzene rings marked "2-4" increases with chain length, with each subsequent ring starting with a smaller NICS value than the ones before. The lowest value is -4.88 ppm which is significantly lower in magnitude than that of benzene's NICS, namely -9.70 ppm. The decrease in the NICS value of the cyclopentadienyl anions as well as the end benzene ring means that the π electrons are less delocalized. This is compensated by the increase in the chemical shift of the inner benzene rings which suggests that the electrons in these rings are more delocalized. It is because of these competing effects that the increase in electron affinities with successive addition of benzene rings slows and tends to saturate.

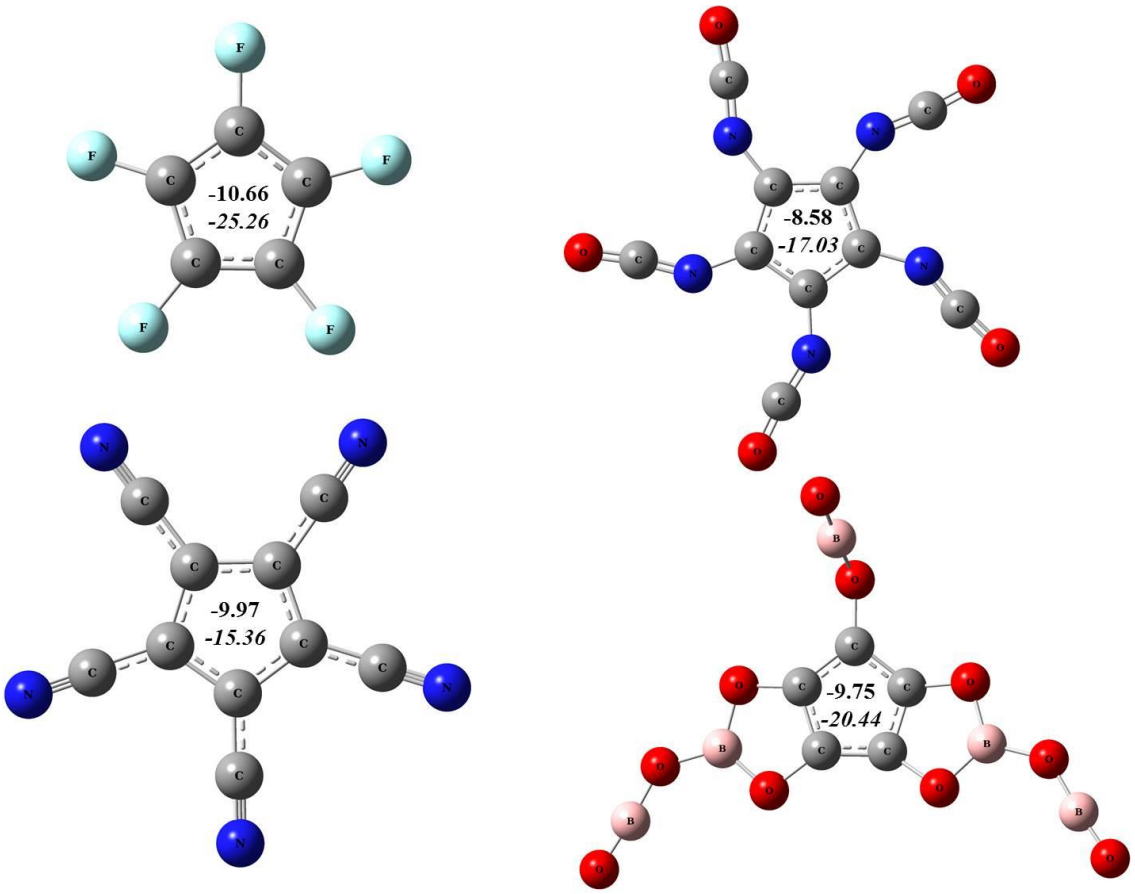

(a)

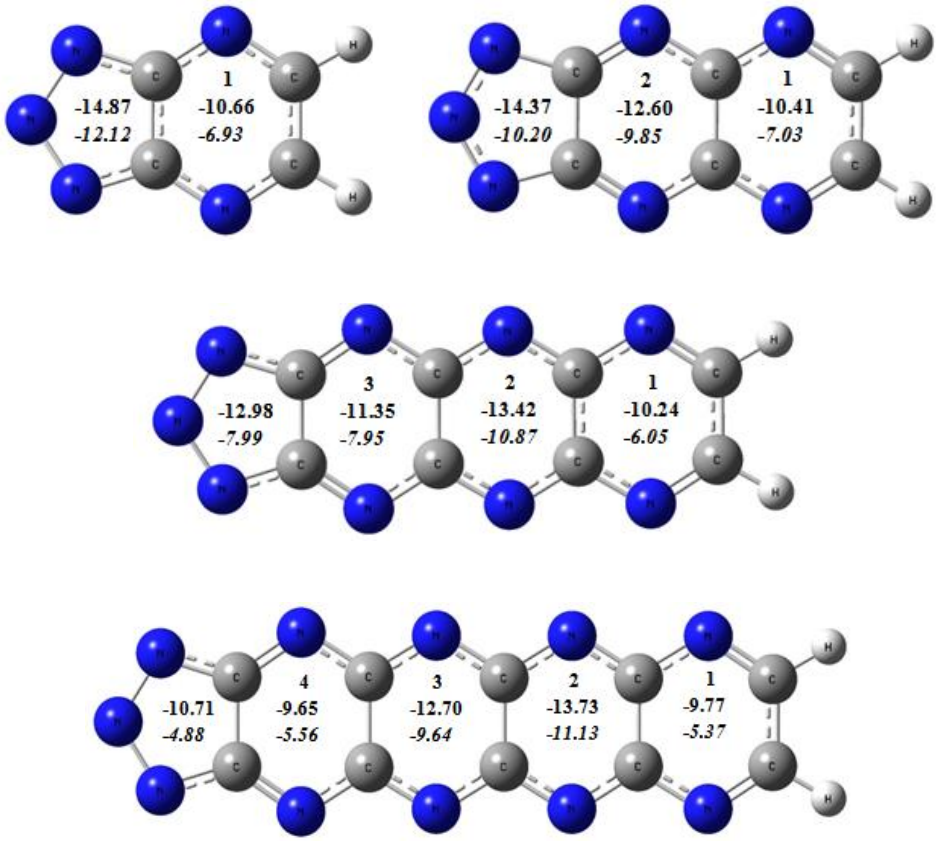

(b)

Fig. 11: NICS values (in ppm) for C_5X_5 (X= F, NCO, CN, BO_2) and first four PAH molecules of Fig. 9. First value is 1 Å above plane, second value, in italics, is in the plane.

3.1.8 Additional information

Calculations for C_6X_6 (X= F, CN, BO_2) were carried out with the final geometries and EA values shown in Fig. 19. As the C_6X_6 neutral already satisfies Huckel's rule the addition of an electron removes this stability and so both the F and BO_2 substitutions still result in a low EA, though still improved over the EA of benzene. In the case of the CN substitution the EA is pseudohalogen in nature, which is attributed to the high electron withdrawing property of CN. It is this property in combination with the EA of cyclopentadiene that led to such high EA in that case.

The ground state geometries of F ligand substituted flourene and benz[*f*]indene were calculated for the neutral and anionic systems. They had lower EA than their N core substituted counterparts so were not of importance, but have been included here for the sake of completeness. Here the lowest energy for both neutral and anion were for the flourene structure

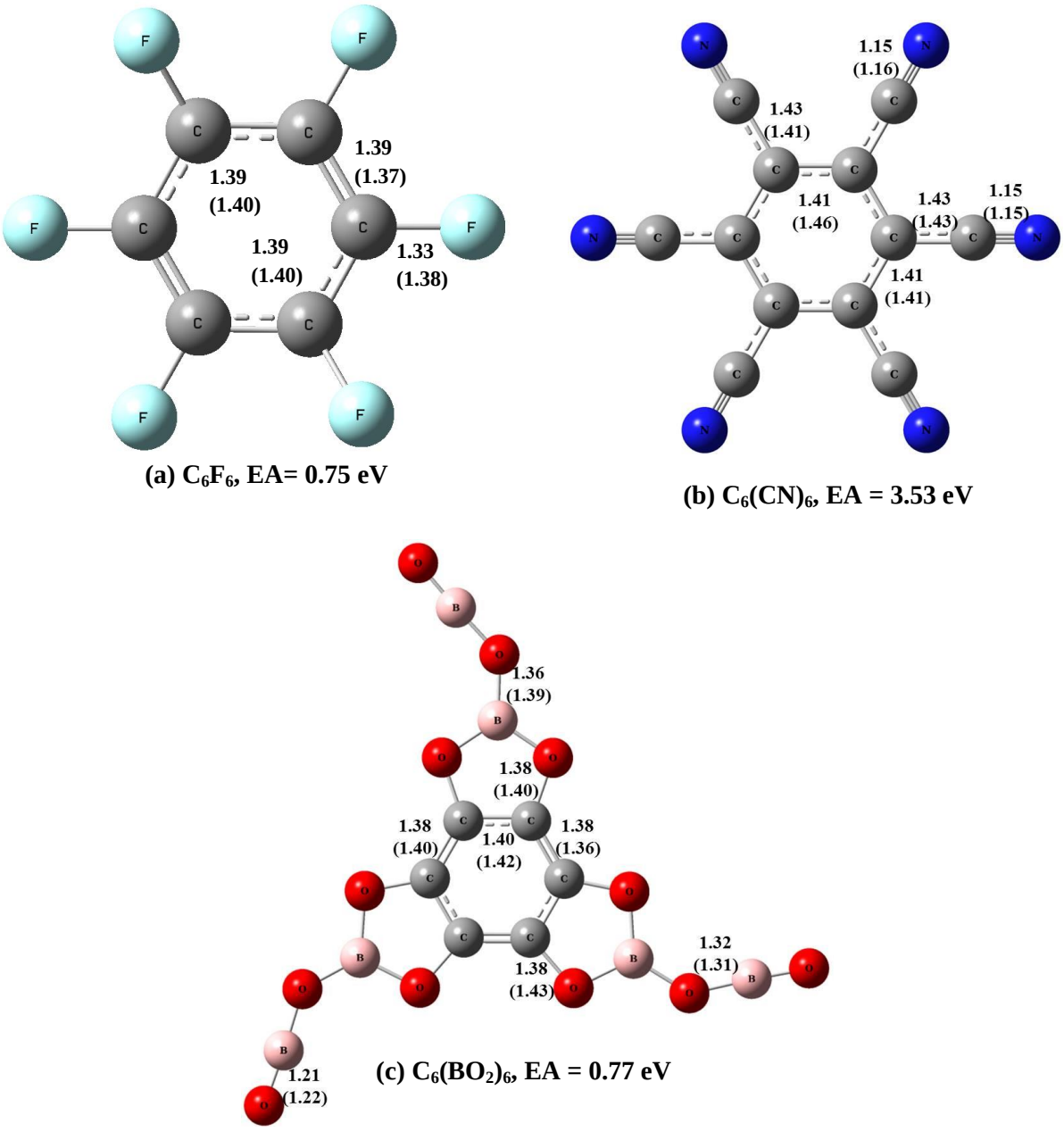

(a) C_6F_6, EA= 0.75 eV

(b) $C_6(CN)_6$, EA = 3.53 eV

(c) $C_6(BO_2)_6$, EA = 0.77 eV

Fig. 12: Equilibrium geometries of the ground state of neutral and anionic C_6X_n (n=6; X= F, CN, BO_2). The bond lengths are given in Å. The bond lengths in brackets are those of the anion.

with the benz[*f*]indene structure being a low level isomer with the energy difference ΔE shown in Fig. 13 along with the bond lengths. We see that the isomer maintains a higher EA than the ground state; however both are lower than the EA of C_4N_9 (4.58eV) by at least 1.60eV, and thus the reason for their being discarded from the main discussion.

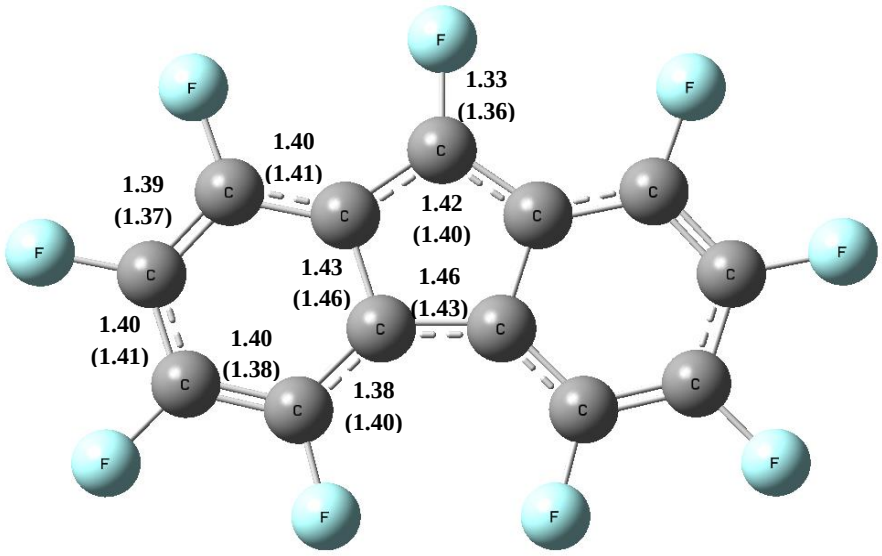

(a) $C_{13}F_9$, Flourene, EA 2.87 eV

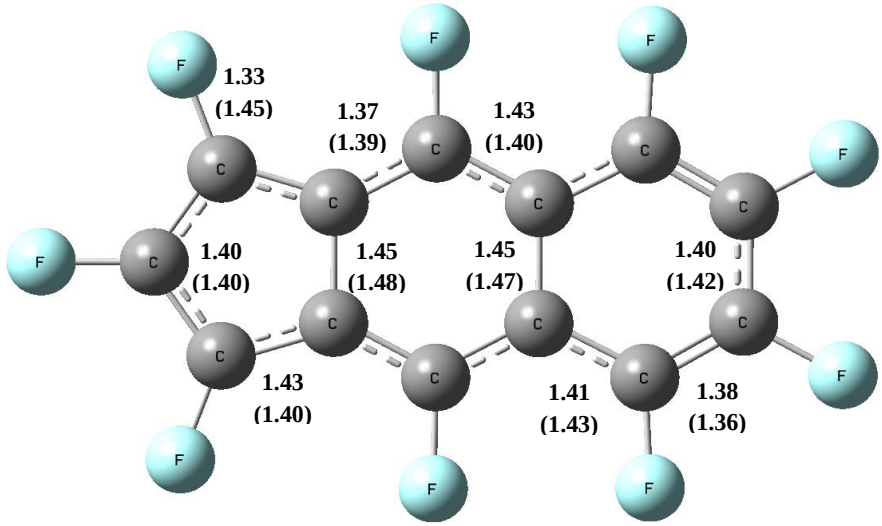

(b) $C_{13}F_9$, Benz[*f*]indene, ΔE= 0.47 eV, EA=2.98 eV

Fig. 13: Geometries of $C_{13}F_9$. The bond lengths are given in Å. The bond lengths in brackets are those of the anion.

3.2 Results and discussion of induction of superhalogen behavior in organic molecules

We begin our discussion with cyclopropenyl cation ($C_3H_3^+$). The optimized geometries of BC_2H_3 and $[B_2CY_3]^-$ (Y=H, F, CN) along with their equilibrium distances are given in Figure 14. It is evident form the figure that all these molecules are planar. As mentioned before $C_3H_3^+$ is a 2π electronic system which makes it aromatic. Substitution one C by B leaves neutral BC_2H_3 still a 2π system. The calculated EA value of this molecule is -1.09 eV. As expected one more B substitution in the ring increases the EA to +1.70 eV. However, it does not make it a superhalogen by itself. We next substituted the H atoms with more electronegative F and CN moieties. This makes the EA to rise even further reaching a value of 2.98 eV for B_2CF_3 and 4.66 eV for $B_2C(CN)_3$, the latter being a superhalogen!

The Optimized geometries of anionic XC_5H_6 (X = B, Al, Ga) molecules along with their equilibrium distances are given in Figure 15. The calculated electron affinities (EA), vertical detachment energies (VDE) and nucleus independent chemical shift (NICS) values of these molecules are given in Table 4.

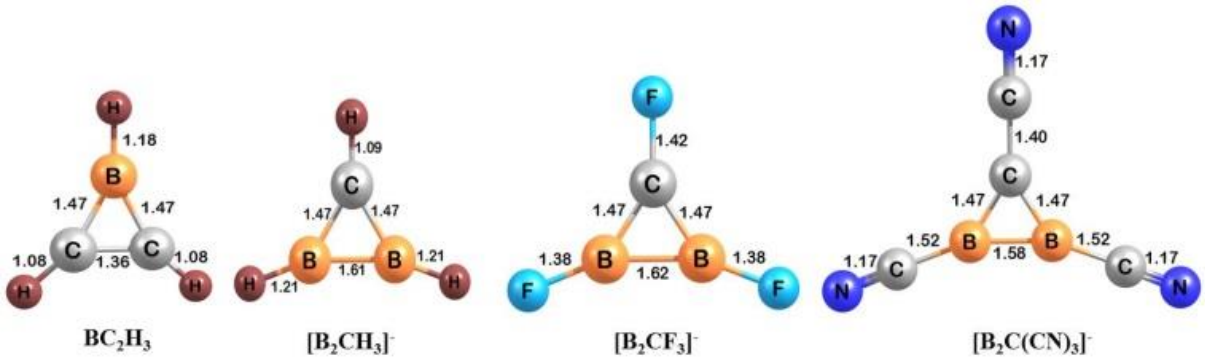

Fig. 14: Optimized geometries of BC_2H_3, $[B_2CH_3]^-$, $[B_2CF_3]^-$, and $[B_2C(CN)_3]^-$

At the DFT/B3LYP level of theory the calculated EA of benzene (C_6H_6) is -1.30 eV which is in good agreement with the experimental value of -1.15 eV. When one C is replaced by B, Al, or Ga the EAs change substantially and become positive. This is because replacement of tetravalent C atom in C_6H_6 by trivalent B, Al or Ga causes the molecule to have 5π electrons which is one electron short off fulfilling the aromaticity rule. To gain stability XC_5H_6 needs one more electron to become a 6π electronic system. Thus, the electron affinity increases.

Note that the EA of XC_5H_6 decreases from 2.27 eV to 1.79 eV as we move down the group from B to Al to Ga. This is because the increase in size of X causes the C-X bond length to increase, resulting in less charge transfer between C and X. Even though the EA and VDE values of XC_5H_6 (X = B, Al, Ga) given in Table 4 are substantially higher than that of C_6H_6, the molecules are *not* superhalogens.

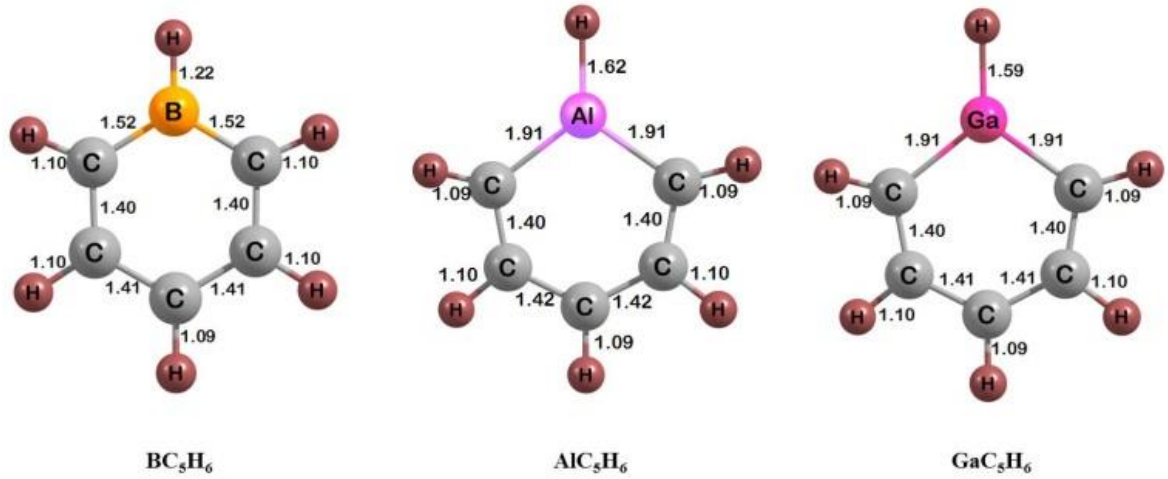

Fig. 15: Optimized geometries of anionic XC_5H_6 (X = B, Al, Ga)

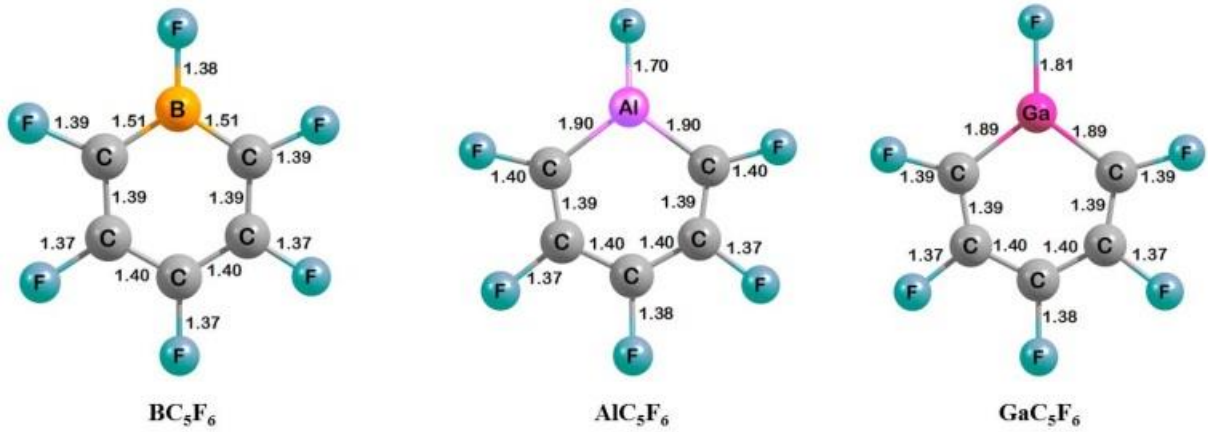

Fig. 16: Optimized geometries of anionic XC_5F_6 (X = B, Al, Ga)

We next replaced the H atoms in XC_5Y_6 (X = B, Al, Ga) by Y=F and CN moieties. The optimized anion geometries are given in Figures 16 and 17 for Y=F and CN, respectively. Note that in the case of CN moiety either C or N can bind to the B (Al, Ga) atom. The most stable geometry is the one when C of CN moiety binds to the metal atom. The corresponding EA and VDE values are given in Table 4. Incorporation of F makes EA values increase over that of the un-substituted molecule, but XC_5F_6 (X = B, Al, Ga) molecules are still *not* superhalogens. The situation is changed when we use CN as a ligand. Substitution of CN does not affect the ring geometry, but allows $XC_5(CN)_6$ (X = B, Al, Ga) molecules to have electron affinities as high as 5.87 eV, making all of them superhalogens. The reason CN substitution works well over the F substitution to produce an organic superhalogen can be attributed to the strong electron withdrawing power of CN. Note that the electron affinity of CN is 3.86 eV[50] while that of F is 3.4 eV. This shows that with proper replacement of C and H, an organic molecule can become a superhalogen!

To demonstrate that these molecules are aromatic, we have calculated the chemical shift at the center and 1Å above the center by employing Nucleus Independent Chemical Shift (NICS) method.

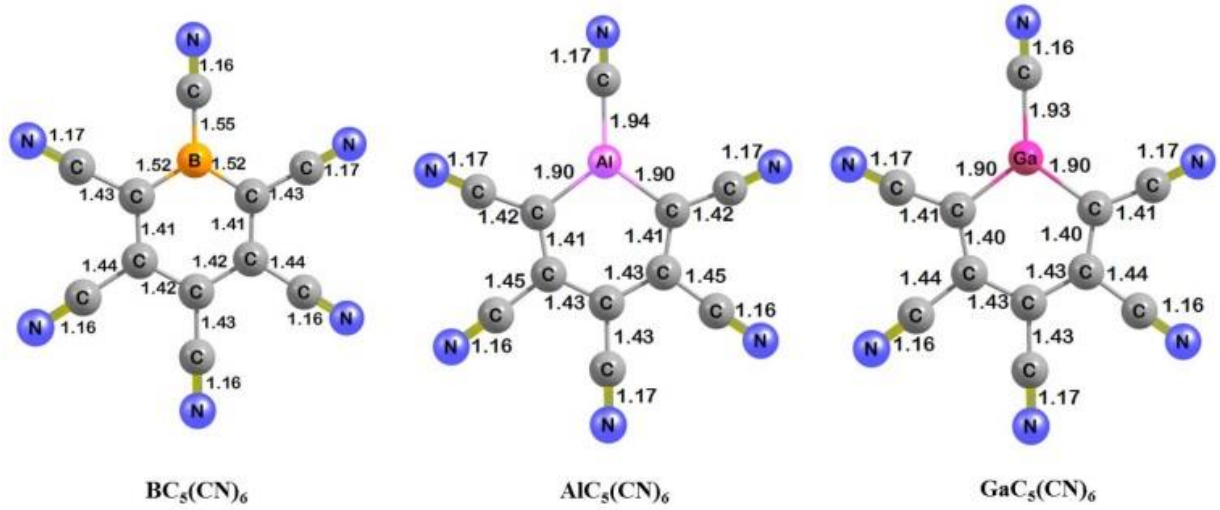

Fig. 17: Optimized geometries of anionic $XC_5(CN)_6$ (X = B, Al, Ga)

These values are identified as NICS(0) and NICS(1), respectively. We see that all these molecules are aromatic due to their negative NICS values. Although π electron delocalization is disturbed when C in C_6H_6 is replaced by X (X= B, Al, Ga) as reflected by their NICS values (Table 4), they still behave like aromatic molecules because of the presence of charge separation on C-X bond, making electrons delocalized over the ring. From NBO charges we indeed find that there is charge distribution on the C-X bond. This becomes clear when we examine the HOMO-4 molecular orbital of C_6H_6 as well as those of XC_5H_6 (X = B, Al, Ga) depicted in Figure 18. Ligands like F and CN makes the ring even more aromatic than C_6H_6 (Table 4).

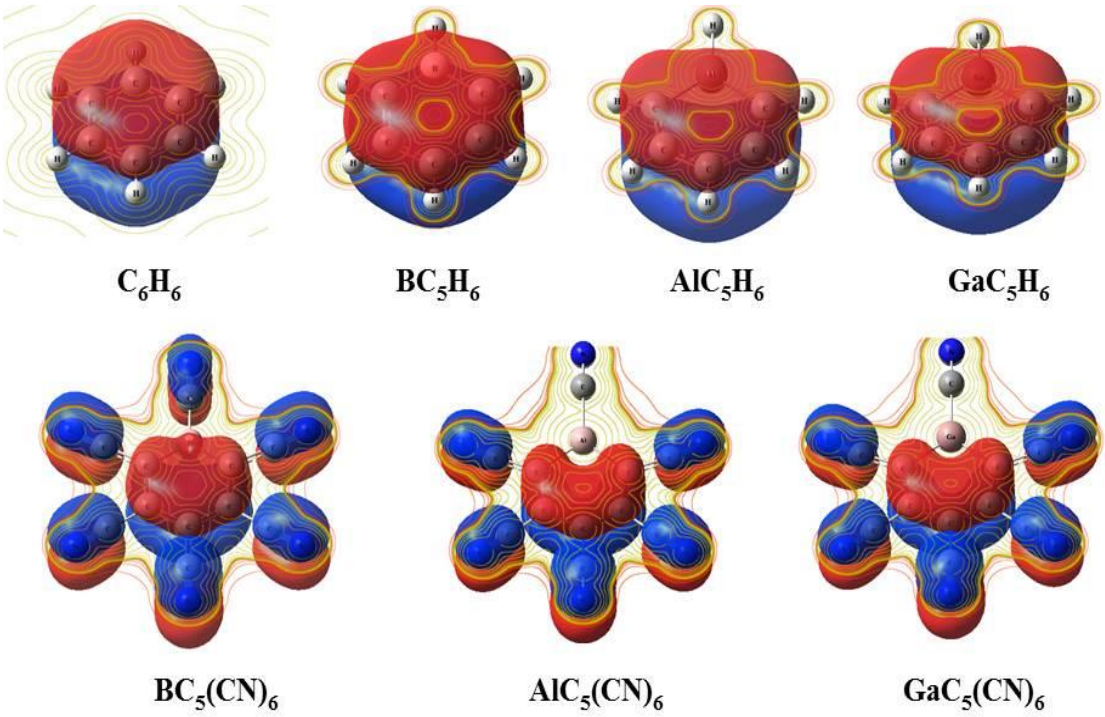

Fig. 18: HOMO-4 Molecular Orbital of C_6H_6 , XC_5H_6 (X = B, Al, Ga) and HOMO-3 Molecular Orbital of $XC_5(CN)_6$ (X = B, Al, Ga) Reflecting π Electron Cloud.

Table 4: Calculated EA, VDE and NICS (0/1) for Different 2π and 6π Electronic Systems at B3LYP/6-31+G(d,p) level of theory.

Systems	EA(eV)	VDE(eV)	NICS(0) (ppm)	NICS(1) (ppm)
BC_2H_3	-1.09	-1.08	-18.94	-13.99
B_2CH_3	1.70	2.39	-16.70	-14.27
B_2CF_3	2.98	3.92	-38.66	-10.89
$B_2C(CN)_3$	**4.66**	**5.32**	**-23.28**	**-13.34**
C_6H_6	-1.30	-1.10	-8.12	-10.19
BC_5H_6	2.27	2.35	-5.85	-7.85
BC_5F_6	3.19	3.49	-17.47	-10.87
$BC_5(CN)_6$	**5.87**	**5.93**	**-8.71**	**-8.40**
AlC_5H_6	1.79	1.84	-4.00	-5.23
AlC_5F_6	2.70	2.92	-15.00	-9.57
$AlC_5(CN)_6$	**5.21**	**5.27**	**-6.58**	**-5.82**
GaC_5H_6	1.85	1.91	-4.20	-5.81
GaC_5F_6	2.88	3.11	-15.43	-9.95
$GaC_5(CN)_6$	**5.31**	**5.36**	**-6.83**	**-6.30**

To examine if there is a critical number of CN molecules that is required before metal substituted C in C_6H_6 can be a superhalogen, we focused on $BC_5H_{6-m}(CN)_m$ (m= 0-6). For each value of m we have calculated the equilibrium geometry of neutral and anionic $BC_5H_{6-m}(CN)_m$ molecules and determined their EAs and VDEs. NICS method was used to calculate their aromaticity. The variation of VDE and NICS values as function of CN ligands are given in Figure 19. We see that with gradual substitution of H with CN the VDEs of $BC_5H_{6-m}(CN)_m$ molecules rise, reaching the superhalogen value at m=2. The NICS values also rise with VDE and the molecules become increasingly aromatic. The highest values of VDE and NICS(0), namely, 5.93 eV and -8.71 ppm are reached for $BC_5(CN)_6$.

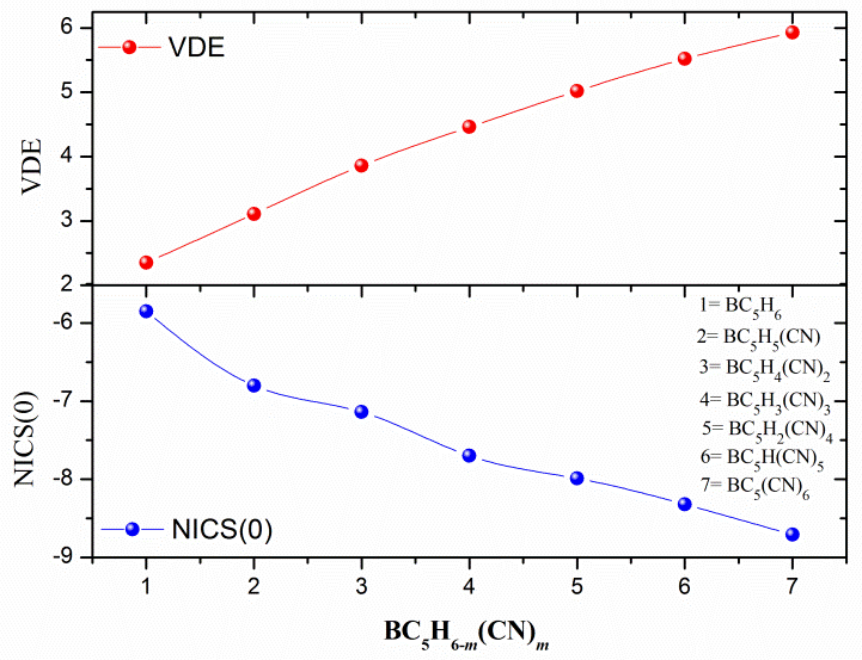

Fig. 19: Variation of VDE and NICS upon gradual CN substitution in BC_5H_6

Note that the NICS(0) value of $BC_5(CN)_6$ is even higher than that of C_6H_6, namely, -8.12 ppm. However, the NICS(1) value (-8.40 ppm) of $BC_5(CN)_6$ is lower than that (-10.17 ppm) of C_6H_6. This is understandable because the B atom in the ring decreases the π electron delocalization.

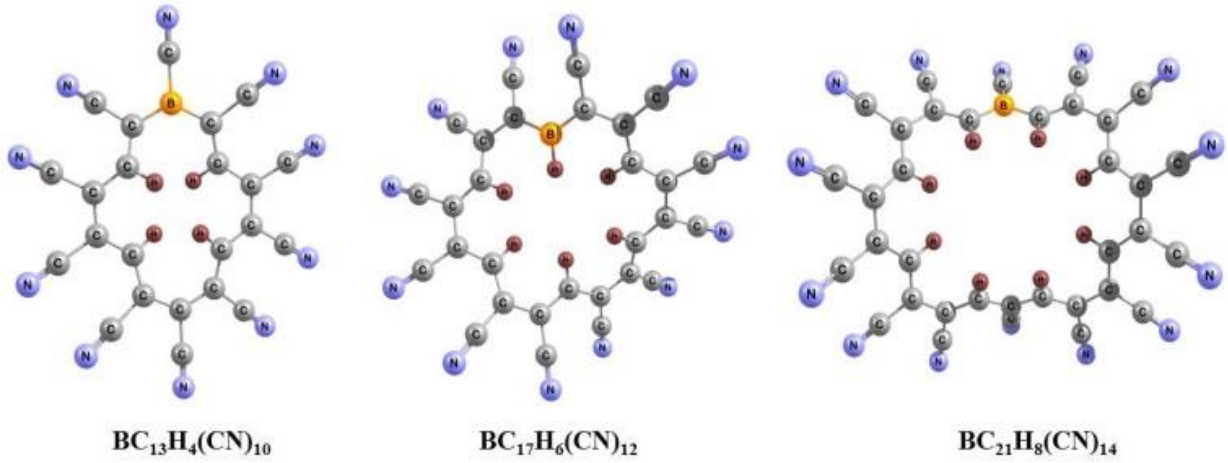

Fig. 20: Optimized geometries of anionic $BC_{13}H_4(CN)_{10}$, $BC_{17}H_6(CN)_{12}$ and $BC_{21}H_8(CN)_{14}$

We know that higher π systems such as $C_{14}H_{14}$, $C_{18}H_{18}$, and $C_{22}H_{22}$ annulene molecules are aromatic because they too obey $(4n+2)$ π (n= 3, 4 and 5) aromaticity rule. We follow the same procedure depicted in schemes 1 and 2 to see if these molecules can also be made superhalogens. We found that the simultaneous substitution of one C by B in the ring and H atoms with CN moieties makes $BC_{13}H_4(CN)_{10}$, $BC_{17}H_6(CN)_{12}$ and $BC_{21}H_8(CN)_{14}$ (Figure 20) to have VDE values 5.91 eV, 5.88 eV and 5.95 eV, respectively. This finding again confirms their superhalogen behavior. We point out that in spite of their superhalogen behavior these molecules are no longer aromatic because they are non-planar due to CN substitution.

3.3 Continuing work: Metallo-organic hyperhalogens?

If a traditional hyperholgen is made from attaching k+1 ligands to a metallic atom with a valence of k, then it should be possible to use the superhalogens in sections 3.1 and 3.2 as ligands in the formation of a hyperhalogen. Ongoing research is exploring the possibility of these metallo-organic hyperhalogens existing as stable or meta-stable molecules with large EA. Several possible superhalogens are being tested with the form MX_y where, M=Li, Mn, Mg, Al, and Zn; X =C_4H_4N, $C_3H_3N_2$, $BC_5(CN)_6$, and $C_4H_2N_5$; y=1-(k+1). As the number of ligands, y, is being varied from 1 to k+1, the onset of hyperhalogen behavior can be examined. Further tests to guarantee that all structures exist on the potential energy surface will be conducted as well.

Conclusion

Electron counting rules have played a major role in the design and synthesis of a large number of superhalogens over the past 30 years and these superhalogens have the potential to lead to new salts as well as to new chemistry. Among these rules, the octet rule applies to light atoms with atomic number less than 20, the 18-electron rule applies to molecules containing transition metal atoms, and the Wade-Mingos rule applies to electron deficient moieties such as borane-derivatives. It has been shown that molecules that require only one extra electron to satisfy the above rules can have large electron affinities. However, no organic molecule that satisfies the aromaticity rule when one extra electron is added has been shown to mimic a halogen, let alone behaving as a superhalogen. Using density functional theory and hybrid functional (B3LYP) for exchange-correlation potential we have studied the geometries, electronic structure, thermal stability, vertical detachment energies, electron affinities, adiabatic detachment energies, and aromatic properties of a number of molecules formed by either by tailoring the ligands of cyclopentadienyl or by multiple benzo-annulations of cyclopentadienyl in conjunction with the substitution of CH groups with isoelectronic N atoms.

These methods allowed the creation of aromatic superhalogens with electron affinities as high as 5.12-5.59 eV. These molecules consist of the formula C_5X_5 (X=CN, CF_3) and $C_{4+2n}N_{5+2n}H_2$ (n = 0 – 5). Both methods mentioned above show promise in creating superhalogens; the first method leads to higher EA, while the second can be tailored to yield

electron affinity of almost any desired value by altering chain length and N substitution sites. Thermal stability of these new species has been further examined by calculating the energies necessary to fragment these molecules using pre-determined fragmentation pathways. The Nucleus Independent Chemical Shift (NICS) method was used to confirm the aromaticity of these anions.

A second method demonstrated that organic superhalogens can be created frome benzene by replacing C atoms with B and H ligand atoms with CN moieties. Core atom substitution alone, however, is not sufficient to make these molecules a superhalogen. For this to happen, the ligands have to have higher electron affinity than F. The aromaticity rule is seen to play an important role in the design of these organic superhalogens.

This study provides new possibilities for the synthesis of organic superhalogens as wells as new insight into the mechanisms through which Huckel's rule of aromaticty plays an important part in their design. Such molecules could lead to new salts as well as new organic catalysts.

List of References

[1] G. Gutsev, A. I. Boldyrev, *Chem. Phys.* **1981**, *56*, 277–283.
[2] G. Gutsev, A. I. Boldyrev, *Adv. Chem. Phys.* **1985**, *61*, 169–221.
[3] C. Kolmel, G. Palm, R. Ahlrichs, M. Bar, A. I. Boldyrev, *Chem. Phys. Lett.* **1990**, *173*, 151–156.
[4] G. Gutsev, A. I. Boldyrev, *J. Phys. Chem.* **1990**, *94*, 2256–2259.
[5] G. Gutsev, A. I. Boldyrev, *Chem. Phys. Lett.* **1983**, *101*, 441–445.
[6] X.-B. Wang, C.-F. Ding, L.-S. Wang, A. I. Boldyrev, J. Simons, *J. Chem. Phys.* **1999**, *110*, 4763–4771.
[7] S. Freza, P. Skurski, *Chem. Phys. Lett.* **2010**, *487*, 19–23.
[8] C. Sikorska, P. Skurski, *Chem. Phys. Lett.* **2012**, *536*, 34–38.
[9] I. Anusiewicz, *J. Phys. Chem. A.* **2009**, *113*, 6511–6516.
[10] A. I. Boldyrev, J. Simons, *J. Chem. Phys.* **1993**, *99*, 4628–4637.
[11] G. L. Gutsev, P. Jena, H. J. Zhai, L.-S. Wang, *J. Chem. Phys.* **2001**, *115*, 7935–7944.
[12] I. Swierszcz, I. Anusiewicz, *Chem. Phys.* **2011**, *383*, 93–100.
[13] S. Smuczynska, P. Skurski, *Inorg. Chem.* **2009**, *48*, 10231–10238.
[14] G. L. Gutsev, B. K. Rao, P. Jena, X. B. Wang, L.-S. Wang, *Chem. Phys. Lett.* **1999**, *312*, 598–605.
[15] G. L. Gutsev, P. Jena, H. J. Zhai, L.-S. Wang, *J. Chem. Phys.* **2001**, *115*, 7935–7944.
[16] S. Behera, D. Samanta, P. Jena, *J. Phys. Chem. A* **2013**, *117*, 5428-5434.
[17] C. Paduani, P. Jena, *J. Nanoparticles Research* **2012**, *14*, 1035-1043.
[18] D. Samanta, M. M. Wu, P. Jena, *J. Inorg. Chem.* **2011**, *50*, 8918-8925.
[19] M. Gotz, M. Willis, A. Kandalam, G. G. Gantefor, P. Jena, *Chem. Phys. Chem.* **2010**, *11*, 853-858.
[20] B. Pathak, D. Samanta, R. Ahuja, P. Jena, *Chem. Phys. Chem.* **2011**, *12*, 2422-2428.
[21] M. Willis, M. Gotz, A. K. Kandalam, G. Gantefor, P. Jena, *Angew. Chem. Int. Ed.* **2010**, *49*, 8966-8970.
[22] M. Marchaj, S. Freza, O. Rybacka, P. Skurski, *Chem. Phys. Lett.* **2013**, *574*, 13–17.
[23] D. Samanta, P. Jena, *J. Am. Chem. Soc. (communications)* **2012**, *134*, 8400-8403.
[24] P. Jena, *J. Phys. Chem. Letters* **2013**, *4*, 1432-1442.
[25] H-J. Zhai, J. Li, L-S. Wang, *J. Chem. Phys.* **2004**, *121*, 8369-8374.
[26] S. Freza, P. Skurski, *Chem. Phys. Lett*. **2010**, *487*, 19-23.
[27] J. Yang, X-B. Wang, X-P. Xing, L-S. Wang, *J. Chem. Phys*. **2008**, *128*, 201102 (1-4).
[28] A. W. Hofmann, *Proceedings of the Royal Scociety.* **1855**, *8*, 1-3.
[29] P. v. R. Schleyer, *Chemical Reviews.* **2001**, *101*, 1115–1118.
[30] E. Hückel, *Z. Phys*. **1931**, *70* 204–86.
[31] W. V. E. Doering, F. L. Detert, *J. Am. Chem. Soc*. **1951**, *73*, 876-877.
[32] A. Hirsch, Z. Chen, H. Jiao, *Angew. Chem., Int. Ed. Engl*. **2000**, *39*, 3915–17.
[33] A. I. Boldyrev, L-S. Wang, *Chem. Rev.* **2005**, *105*, 3716-3757.
[34] I. Nenner, G. J. Schulz, *J. Chem. Phys.* **1975**, *62*, 1747-1758.

[35] P. C. Engelking, W. C. Lineberger, *J. Chem. Phys.* **1977**, *67*, 1412-1417.
[36] Born, M.; Oppenheimer, J. R. *Ann. Physik* **1927**, *79*, 361.
[37] Hartree, D. R. *Proc. Cambridge Phil. Soc.* **1928**, *24*, 89.
[38] Fock, V. Z. *Physik* **1928**, *48*, 73.
[39] Slater, J. C. *Phys. Rev.* **1951**, *81*, 385.
[40] Hohkenberg, P.; Kohn, W. *Phys. Rev. B* **1964**, *136*, B864.
[41] Kohn, W.; Sham, L. J. *Phys. Rev.* **1965**, *140*, A1133.
[42] Becke, A. D. *Phys. Rev. A* **1988**, *38*, 3098.
[43] Slater, J. C. *Phys. Rev.* **1930**, *35*, 210.
[44] Boys, S. F. *Proc. R. Soc. (London) A* **1950**, *200*, 542.
[45] G. Chen, Q. Sun, Q. Wang, Y. Kawazoe, and P. Jena, *J. Chem. Phys.* **2010**, *132*, 194306.
[46] NIST Chemestry Webbook. http://webbook.nist.gov/chemistry/ (Aug 2, 2013).
[47] J. M. Gonzales, C. J. Barden, S. T. Brown, P. v. R. Schleyer, H. F. Schaefer III, Q-S. Li, *J. Am. Chem. Soc.* **2003**, *125*, 1064-1071.
[48] P. v. R. Schleyer, C. Maerker, A. Dransfeld, H. J. Jiao, N. J. r. V. E. Hommes, *J. Am. Chem. Soc.* **1996**, *118*, 6317−6318.
[49] P. v. R. Schleyer, H. J. Jiao, N. J. r. V. E. Hommes, V. G. Malkin, , O. L. Malkina, *J. Am. Chem. Soc.* **1997**, *119*, 12669−12670.
[50] S. E. Bradforth, E. H. Kim, D. W. Arnold, D. M. Neumark, *J. Chem. Phys.* **1993**, *98*, 800-810.